
On the Convergence of Differentially-Private Fine-tuning: To Linearly Probe or to Fully Fine-tune?

Shuqi Ke

Carnegie Mellon University
shuqik@andrew.cmu.edu

Charlie Hou

Carnegie Mellon University
charlieh@andrew.cmu.edu

Giulia Fanti

Carnegie Mellon University
gfanti@andrew.cmu.edu

Sewoong Oh

University of Washington
sewoong@cs.washington.edu

Abstract

Differentially private (DP) machine learning pipelines typically involve a two-phase process: non-private pre-training on a public dataset, followed by fine-tuning on private data using DP optimization techniques. In the DP setting, it has been observed that full fine-tuning may not always yield the best test accuracy, even for in-distribution data. This paper (1) analyzes the training dynamics of DP linear probing (LP) and full fine-tuning (FT), and (2) explores the phenomenon of sequential fine-tuning, starting with linear probing and transitioning to full fine-tuning (LP-FT), and its impact on test loss. We provide theoretical insights into the convergence of DP fine-tuning within an overparameterized neural network and establish a utility curve that determines the allocation of privacy budget between linear probing and full fine-tuning. The theoretical results are supported by empirical evaluations on various benchmarks and models. The findings reveal the complex nature of DP fine-tuning methods. These results contribute to a deeper understanding of DP machine learning and highlight the importance of considering the allocation of privacy budget in the fine-tuning process.

1 Introduction

Today, many differentially-private (DP) machine learning pipelines proceed in two phases: (1) A model is pre-trained (non-privately) on a public dataset. (2) The model is then fine-tuned on private data, typically using DP optimization techniques such as DP stochastic gradient descent (DP-SGD) and its variants [43, 13, 28, 76, 36]. The non-private pre-training phase is believed to guide model parameters into a favorable region within the loss landscape, thereby facilitating easier local optimization under DP constraints. For example, pre-training a GPT-2 model on public data before privately fine-tuning it has been shown to significantly improve the BLEU score from 24.25 to 63.19, while also reducing the privacy cost (i.e., the DP ϵ parameter) from 41.48 to 6.27 during the private fine-tuning phase [90, 36].

Two common strategies for fine-tuning models (with or without DP) are shown in Figure 1: (1) **full fine-tuning** (FT) updates all parameters of the model, and (2) **linear probing** (LP) freezes the lower layers, and only updates the final linear layer. In the non-DP setting, full fine-tuning is known to exhibit better in-distribution accuracy than linear probing on datasets like ImageNet, CIFAR-10, Ent-30 and Liv-17 with few exceptions¹ [50, 93, 42, 52]. On the other hand, for out-of-distribution tasks, linear probing can sometimes outperform full-finetuning [52].

¹Non-DP linear probing achieves better in-distribution test accuracies on DomainNet [52].

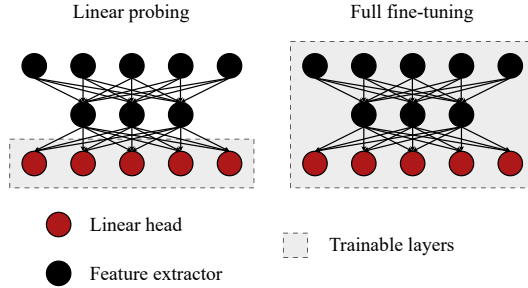


Figure 1: Linear probing freezes the lower layers and optimizes the last linear layer while full fine-tuning optimizes the whole network.

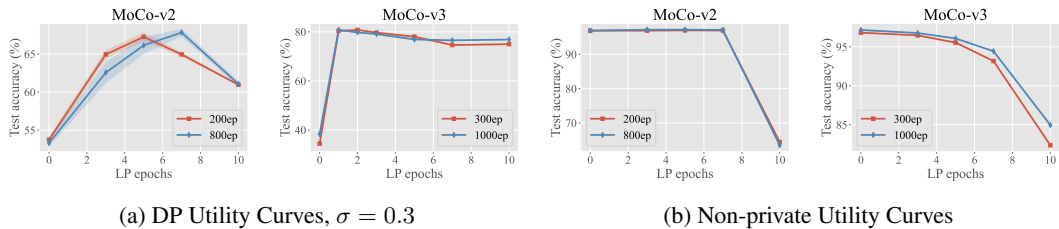


Figure 2: Utility curves for pretraining on ImageNet-1K and fine-tuning on CIFAR-10 over a ResNet-50 model, with pretrained features from MoCo-v2 (left) [21] and MoCo-v3 (right) [22]. The x-axis sweeps the number of LP epochs from 0 to 10; the remaining epochs (out of 10) use full FT. (Top) We observe non-monotonic, concave utility curves for **private** LP-FT, as we sweep the fraction of epochs allocated to LP vs FT, at a noise scale $\sigma = 0.3$. (Bottom) In contrast, the utility curves are monotonic for **non-private** two-phase fine-tuning, with full fine-tuning (leftmost point) performing best.

In the DP setting, Tang et al. [76] have observed empirically that full fine-tuning does not always yield the best test accuracy, even for **in-distribution**² data. Rather, a sequential fine-tuning strategy that starts with linear probing for some epochs, then proceeds with full fine-tuning for the remaining epochs (we refer to this strategy as LP-FT), empirically achieves better test accuracy than either full fine-tuning or linear probing alone [76].

A natural question is whether this phenomenon is generally true for DP machine learning, and if so, *how much* linear probing is enough? In other words, given a total privacy budget, how much should we allocate to linear probing vs. full fine-tuning to achieve the best test accuracy? These questions are currently difficult to answer because we lack a theoretical understanding of the impact of DP fine-tuning on model optimization. Analyzing fine-tuning is challenging because we need to understand the training dynamics, rather than just the loss function and its overall minimizers [68, 52, 83]. Moreover, existing techniques and DP convergence results only consider the dimension of model parameters and ignore the model architecture [37]. We require new theoretical methods that capture the key structural difference between linear probing and full fine-tuning (Figure 1).

In this work, we provide both theoretical and empirical justification for the conjecture that in the DP setting, linear probing followed by full fine-tuning achieves better test loss than linear probing or full fine-tuning alone. We present a theoretical explanation of DP fine-tuning within an overparameterized two-layer linear network. We establish that under certain initial conditions, DP fine-tuning can be less effective than DP linear probing with high-quality pre-trained features. Furthermore, we characterize a non-monotonic and concave utility curve: as one increases the fraction of rounds used for linear probing, test accuracy increases up to a point, then decreases. Figure 2 illustrates this trend on a ResNet-50 architecture; experimental settings are provided in Section 4.2. We observe that for non-private optimization (bottom), full fine-tuning achieves the highest test accuracy. However, for DP-SGD (top), linear probing outperforms full fine-tuning, and LP-FT outperforms both LP and FT.

²In this work, we focus on in-distribution settings. We will just use “test accuracy” rather than “in-distribution test accuracy” in the rest of this paper.

Our theoretical results analyze the convergence of a Langevin diffusion-based model of DP gradient descent (DP-GD). To prove our main results, we introduce to the Langevin diffusion setting the *imbalance matrix*, an invariant previously studied in the context of gradient flows [3, 30, 62, 64, 60]. We prove that in DP fine-tuning, (1) the diagonal of the expected imbalance matrix linearly increases and other entries remain invariant, which is different from the case for (noise-free) gradient flows. (2) However, we find that the expectation of the imbalance matrix is invariant if we scale the DP noise of the linear head with respect to its size. This invariant property of multi-layer networks helps us disentangle the nonconvexity of DP-GD and leads to new utility bounds.

Technically, these tools allow us to bound the convergence rates of both DP linear probing and nonconvex DP full fine-tuning. Unlike prior work in this field, our results do not require convexity conditions, other “model-free assumptions” (e.g. Lipschitz conditions, dissipativity, smoothness, the Poincaré inequality), or approximations (e.g. neural tangent kernel) in DP gradient descent analysis [9, 72, 18, 6, 80, 16, 37, 87]. We believe our analysis techniques may thus be of broader interest.

To summarize, our contributions are:

- **DP Fine-Tuning (FT) vs. Linear Probing (LP):** We provide the first theoretical evidence that DP linear probing can outperform DP full fine-tuning, even on in-distribution data. In particular, our analysis on a two-layer linear network regression task indicates that DP full fine-tuning may underperform relative to linear probing when privacy budgets are low.
- **Two-Phase Sequential Approach (LP-FT):** We analyze a two-phase fine-tuning method, beginning with linear probing and then transitioning to full fine-tuning. Our results theoretically demonstrate a trade-off in allocating the privacy budget between the two phases. Contrary to initial expectations, this sequential approach can outperform mere linear probing, even when pre-trained features are already highly effective.
- **We empirically evaluate the trends predicted by our theoretical model over nonlinear neural networks.** We experiment on four fine-tuning benchmarks (ImageNet-1K→CIFAR-10, ImageNet-1K→STL-10, CIFAR-10→STL-10, RandP→CIFAR-10) and five model architectures (MobileNet-v3, Mini-DeiT, ResNet-18, ResNet-50, WideResNet-16-4). Our results confirm our theoretical predictions, showing that concave utility curves generally exist for deep neural networks on real datasets.

2 Setup and Background

Task and notation. For our theoretical analyses, we consider a regression task with n training data points: $\{(x_i, y_i) : x_i \in \mathbb{R}^d, y_i \in \mathbb{R}\}_{i=1}^n$. We collect the data inputs in a matrix $X \in \mathbb{R}^{n \times d}$ and put the labels in a vector $Y \in \mathbb{R}^n$. The objective is to train a predictor $f : \mathbb{R}^d \rightarrow \mathbb{R}$ that minimizes the empirical risk function $\mathcal{L} = \sum_{i=1}^n (1/2)(f(x_i) - y_i)^2$.

2.1 Differentially-Private Optimization

Differential privacy (DP) is a widely-used method to evaluate privacy leakage in a database accessed through queries [31]. In the context of machine learning, it ensures that an adversary cannot confidently ascertain whether a specific training sample (or set of training samples) was in the training dataset.

Definition 2.1 ((ϵ, δ) -Differential Privacy [31]). We say two datasets $\mathcal{D}, \mathcal{D}'$ with n records each are neighboring if they only differ in one record. Given privacy parameters $\epsilon > 0, \delta \in (0, 1)$, we say a random algorithm \mathcal{A} satisfies (ϵ, δ) -differential privacy if for any measurable $B \subseteq \text{range}(\mathcal{A})$ and for any pair of neighboring datasets $\mathcal{D}, \mathcal{D}'$, we have

$$\mathbb{P}(\mathcal{A}(\mathcal{D}) \in B) \leq e^\epsilon \mathbb{P}(\mathcal{A}(\mathcal{D}') \in B) + \delta \quad (1)$$

where $\mathcal{A}(\mathcal{D})$ denotes the output distribution of algorithm \mathcal{A} on dataset \mathcal{D} .

Definition 2.2 (ℓ_2 sensitivity [31]). Let $g : \mathbb{R}^{n \times d} \rightarrow \mathbb{R}^p$ be a function operating on datasets. Let $D = (X, Y), D' = (X', Y') \in \mathbb{R}^{n \times (d+1)}$ be neighboring datasets. The ℓ_2 -sensitivity of g is defined as $\Delta(g) := \sup_{D \sim D'} \|g(D) - g(D')\|_2$.

The privacy guarantee of Langevin diffusion depends on the ℓ_2 sensitivity of the loss gradients [37, 87].

DP Gradient Descent (DP-GD). DP-GD is a widely-adopted DP variant of Gradient Descent. Each iteration of DP-GD consists of two parts: (1) clipping the gradients of each data point to a prefixed norm of at most C , and (2) adding zero-mean spherical Gaussian noise of a prefixed scale σ to the mean of the clipped gradients [1, 74]. DP-GD is (ϵ, δ) -differentially private if we choose $\sigma = \Omega((C/n)\sqrt{T \log(1/\delta)}/\epsilon)$, where T is the number of iterations [31].

Algorithm 1 Differentially Private Gradient Descent

Require: initial parameter $\theta^{(0)}$, learning rate α , noise scale σ , gradient norm bound C , train data \mathcal{D} , $T \in \mathbb{Z}$.

Output: $\theta^{(T)}$ and compute the overall privacy cost (ϵ, δ) using the Rényi Differential Privacy accountant.

- 1: **for** $t = 0, \dots, T - 1$ **do**
 - 2: $\mathbf{g}^{(t)} \leftarrow \frac{1}{n} \left(\sum_{(x_i, y_i) \in \mathcal{D}} \text{clip}_C(\nabla_w \ell(w^{(t)}, x_i, y_i)) \right)$
 - 3: $\mathbf{g}^{(t)} \leftarrow \mathbf{g}^{(t)} + \mathcal{N}(0, \sigma^2 \mathbf{I})$
 - 4: $\theta^{(t+1)} \leftarrow \theta^{(t)} - \alpha \mathbf{g}^{(t)}$
 - 5: **end for**
-

Langevin Dynamics. A Langevin diffusion is a stochastic differential equation that models the dynamics of a system under the influence of both deterministic and fluctuating forces, also known as random forces [54]. For example, we can define an m -dimensional Langevin diffusion to model DP-GD as follows:

$$\partial \theta(t) = -\nabla \mathcal{L}(\theta(t)) \partial t + \sqrt{2\sigma^2} \partial W(t) \quad (2)$$

where $\theta \in \mathbb{R}^m$ is the model parameter evolving in continuous time, \mathcal{L} is the empirical risk, $\sigma > 0$ is the noise scale, and $\{W(t)\}_{t \geq 0}$ is the standard Brownian motion in \mathbb{R}^m . This Langevin diffusion has been used for the analysis of gradient-based stochastic learning algorithms like DP-(S)GD [85, 55, 25, 87, 37]. Notice that (2) captures the additive noise of DP-GD, but it does not capture the effect of gradient clipping. Like prior work [85, 25, 37, 87], we do not explicitly model clipping. Instead, we have assumed the noise scale is upper bounded in Assumption 3.4; other works typically handle this issue by assuming Lipschitz conditions or making analogous assumptions upper bounding the gradient norm [72, 37].

3 Theoretical Analysis

3.1 Linear overparameterized setting

Model. We focus on a setting adapted from prior works that utilizes pre-trained representations [4, 77, 52, 64]. We define a two-layer linear network as function $f : \mathbb{R}^d \rightarrow \mathbb{R}$, $f(x) = \langle v, Bx \rangle$ where $v \in \mathbb{R}^k$, $B \in \mathbb{R}^{k \times d}$. Then we can write the empirical risk function as

$$\mathcal{L}(v, B) = \frac{1}{2} \|XB^T v - Y\|_2^2. \quad (3)$$

For simplicity, we assume that $n \geq d$ and $X^T X = I_{d \times d}$. Note that the loss function is nonconvex in the parameters being fine-tuned, so the gradient-descent training becomes a nonlinear dynamical system. This significantly complicates theoretical analysis [64]. Prior works have dealt with this challenge by using heavy approximations based on neural tangent kernel and first-order Taylor expansions [16, 87]. We overcome the theoretical difficulties by using conservation laws and geometric properties of Langevin dynamics. We introduce the *imbalance matrix*, an invariant previously studied in the context of gradient flows, to Langevin diffusion [3, 30, 62, 64, 60].

Pretrained features. We evaluate a feature extractor B by the least square error $\gamma(B) := \min_{u \in \mathbb{R}^k} \mathcal{L}(u, B) = Y^T (I_n - XB^T (XB^T)^\dagger) Y$, where $(\cdot)^\dagger$ denotes the pseudo inverse of a matrix. This metric measures the optimal loss we can obtain by linear probing when fixing the current features. We denote the pretrained feature extractor as B_0 . We use γ as shorthand for the initial least square error of our pretrained feature extractor, i.e., $\gamma(B_0)$. We follow the common assumption in prior works [79, 52] and suppose B_0 has orthonormal rows.

Fine-tuning methods. To analyze different fine-tuning approaches, we use Langevin diffusion. Langevin diffusion is a continuous generalization of DP-GD [52]. It has been extensively studied

as a way to understand SGD and its variants [17, 23, 85, 25, 37, 87]. Compared to discrete time-step analysis of SGD, continuous schemes like Langevin diffusion (1) are amenable to theoretical analysis; and (2) provide a more systematic way to analyze and understand a variety of algorithms [75, 55, 32, 52, 65]. Based on previous works [33, 24, 66, 34, 7, 96, 48, 69, 67], we define the Langevin diffusion for linear probing and full fine-tuning below.

Definition 3.1 (Langevin diffusion for linear probing). Let W_t be the standard k -dimensional Brownian motion. Then the Langevin diffusion for linear probing is defined by the following stochastic differential equation:

$$\begin{aligned}\partial v &= -\nabla_v \mathcal{L}(v, B_0) \partial t + \sqrt{2\sigma^2} \partial W_t \\ &= -B_0 X^T (X B_0^T v - Y) \partial t + \sqrt{2\sigma^2} \partial W_t.\end{aligned}\quad (4)$$

Here we use “ ∂ ” as the differential notation.

Definition 3.2 (Langevin diffusion for fine-tuning). Let W_t be the standard k -dimensional brownian motion and W'_t be a matrix whose entries are standard and independent brownian motions. Then we define the Langevin diffusion for fine-tuning a two-layer linear network as

$$\begin{aligned}\partial v &= -\nabla_v \mathcal{L}(v, B) \partial t + \sqrt{2\sigma^2} \partial W_t \\ &= -B X^T (X B^T v - Y) \partial t + \sqrt{2\sigma^2} \partial W_t \\ \partial B &= -\nabla_B \mathcal{L}(v, B) \partial t + \sqrt{2\sigma^2} \partial W'_t \\ &= -v (X B^T v - Y)^T X \partial t + \sqrt{2\sigma^2} \partial W'_t.\end{aligned}\quad (5)$$

Assumptions. We introduce two assumptions for our analysis. The first assumption models the widely-used random initialization of neural network parameters.

Assumption 3.3 (Random initialization of linear head [40]). Initialize the linear head according to a normal distribution $v_0 \sim \mathcal{N}(0, \beta I_{k \times k})$ where $\beta > 0$.

The second assumption is based on the first one. It describes a common phenomenon in differential privacy deployment: the loss might not converge if the privacy mechanism perturbs the gradients too much. To ensure that DP-GD works for full fine-tuning, we assume that the noise scale (or variance) in the privacy mechanism is upper bounded by a constant.

Assumption 3.4 (Upper bounded noise scale). Let $\beta > \frac{-\|X^T Y\| + \sqrt{\|X^T Y\|^2 + 4(1+d)\|X^T Y\| + 4d}}{2k}$. Then we assume that the noise scale $\sigma > 0$ we add for privacy in the fine-tuning process is upper-bounded by

$$\sigma^2 < \min \left\{ \frac{k\beta + \|B_0 X^T Y\|^2}{2k}, \frac{k\beta - 1}{\sqrt{2}(1+d)}, \frac{1}{1 + \sqrt{2}(1+d)} \left[\frac{k\beta(k\beta + \|X^T Y\|^2)}{(1+d)\|X^T Y\| + d} - 1 \right] \right\} \quad (6)$$

By lower bounding β and upper bounding σ , we ensure that the signal of the gradient is significant enough so that the loss is more likely to decrease in full fine-tuning.

3.2 Structural invariance of linear networks

To understand the properties of a dynamics analysis problem, it can be useful to identify *invariants*, or functions whose output is conserved during optimization. Such conservation laws can be seen as a “weaker” form of implicit bias, helping to elucidate which properties (e.g., sparsity, low-rank) are preferred by the optimization dynamics among a potentially infinite set of minimizers [60]. To prove the convergence of our optimization, we study the *imbalance matrix*, an invariant for multi-layer linear networks. The imbalance matrix has previously been studied in the context of gradient flows [3, 30, 62, 64, 60]. However, it has not, to the best of our knowledge, been used in the context of Langevin dynamics.

Definition 3.5 (Imbalance matrix). For a two-layer linear network, we define the imbalance matrix as

$$D := vv^T - BB^T. \quad (7)$$

Prior work on gradient flows has found that the imbalance matrix remains invariant over the evolution of gradient flows modeling gradient descent [3, 30, 60]. This property can be used to derive tight convergence bounds [62, 64]. However, a similar analysis has not materialized for Langevin diffusion models of DP-GD.

We observe that prior work on Langevin diffusion to analyze private optimization has implicitly assumed that the sensitivity of each layer in a neural network is the same [37, 87]. Hence, they fix a uniform noise scale for every parameter of the network. Under these conditions, we show that, when we ignore the sensitivity of each layer and use a uniform noise scale σ , the imbalance matrix is *not* invariant in expectation, unlike in (noise-free) gradient flow [3, 30, 60]. This complicates the use of the imbalance matrix for theoretical analysis [88].

Lemma 3.6 (Imbalance matrix in fine-tuning)

During fine-tuning (Equation (5)), the derivative of the imbalance matrix D in Definition 3.5 is

$$\frac{\partial}{\partial t} \mathbb{E}[D] = (1 - d)\sigma^2 I_{k \times k}, \quad (8)$$

where d is the dimension of data inputs ($B \in \mathbb{R}^{k \times d}$).

Our main observation is that by modeling differences in sensitivity of different layers, we can recover the invariance property of the imbalance matrix. The following proposition characterizes the sensitivity of the linear head and the feature extractor, and illustrates why they have differing sensitivities at initialization.

Proposition 3.7

We assume that the training dataset $\mathcal{D} = (X, Y)$ is normalized such that $X^T X = I_{d \times d}$, $\|Y\|_2 = 1$. We initialize the linear head by $v_0 \sim \mathcal{N}(0, \beta I_{k \times k})$ and $\beta = k/\sqrt{d}$. At the initialization of full fine-tuning, the linear head v has a greater sensitivity than the feature extractor B :

$$\Delta(\nabla_v \mathcal{L}(v_0, B_0)) = \Theta\left(\sqrt{d} \cdot \Delta(\nabla_B \mathcal{L}(v_0, B_0))\right) \quad (9)$$

Based on this observation, we propose a modified version of Langevin diffusion for full fine-tuning, which accounts for layer-wise sensitivity. With this modified definition, the imbalance matrix is again invariant in expectation.

Definition 3.8 (Modified Langevin diffusion for fine-tuning). Let W_t be the standard k -dimensional brownian motion. Let W'_t be a $k \times d$ matrix whose entries are standard and independent brownian motions. Then we define the modified Langevin diffusion for fine-tuning a two-layer linear network as

$$\begin{aligned} \partial v &= -\nabla_v \mathcal{L}(v, B) \partial t + \sqrt{2\sigma^2 d} \partial W_t \\ &= -BX^T X(B^T v - X^T Y) \partial t + \sqrt{2\sigma^2 d} \partial W_t \\ \partial B &= -\nabla_B \mathcal{L}(v, B) \partial t + \sqrt{2\sigma^2} \partial W'_t \\ &= -v(XB^T v - Y)^T X \partial t + \sqrt{2\sigma^2} \partial W'_t. \end{aligned} \quad (10)$$

The only difference between this diffusion and Equation (5) is the additional factor of d , shown in **red**, reflecting the fact that the linear head has greater function sensitivity than the feature extractor.

Lemma 3.9 (Imbalance matrix in the modified fine-tuning dynamics)

In the modified fine-tuning dynamics (Equation (10)), the derivative of the imbalance matrix D in Definition 3.5 is zero in expectation

$$\mathbb{E} \left[\frac{dD}{dt} \right] = 0. \quad (11)$$

As a result, the expected value of the imbalance matrix is a constant in the fine-tuning process.

Note that by modeling the different sensitivities of different layers, we are also modeling a slightly different variant of DP-GD, which applies different noise scales to different layers. This approach has been used successfully in practice, though it is not the most common variant of DP-GD [27].

3.3 Convergence of fine-tuning methods

Theorem 3.10 (Convergence of linear probing)

For simplicity, we assume that $X^T X = I_{d \times d}$. If Assumption 3.3 holds and we run linear probing for time t , then the loss at time t satisfies:

$$\mathbb{E}[\mathcal{L}_{\text{lp}}(t)] \leq \frac{1}{2}(k\beta + \|Y\|^2)e^{-t} + (\gamma + k\sigma^2)(1 - e^{-t}) \quad (12)$$

where k is the dimension of the linear head and γ denotes the least square error of the pretrained feature extractor B_0 . Equation (12) upper monotonically decreases in time if Assumption 3.4 also holds.

The first coefficient $\frac{1}{2}(k\beta + \|Y\|^2)$ in Equation (12) is the initial loss that depends on the random initialization and the training data. In particular, notice that the initial loss does not depend on our choice of B_0 ; this is due to looseness in our analysis; which considers a worst-case initialization. The second coefficient $\gamma + k\sigma^2$ depends on the noise scale σ and the minimum loss γ linear probing could achieve when we fix the feature extractor. The first term $\frac{1}{2}(k\beta + \|Y\|^2)e^{-t}$ describes that the loss tends to exponentially decrease, while the second term describes the limiting behavior induced by linear probing and the added noise.

Theorem 3.11 (Convergence of fine-tuning)

For simplicity, we assume that $X^T X = I_{d \times d}$. If Assumption 3.3 and 3.4 hold, and we run fine-tuning (Equation (10)) for time t , then the loss converges:

$$\mathbb{E}[\mathcal{L}(t)] \leq \frac{1}{2}(k\beta + \|Y\|^2)e^{-ct} + L^\square(1 - e^{-ct}) \quad (13)$$

$$\text{where } \begin{cases} c = k\beta - 1 - \sqrt{2}\sigma^2(1 + d) > 0 \\ L^\square = \sigma^2 \frac{(1+d)\|X^T Y\| + d}{c} \end{cases}.$$

This upper bound has a similar form to Equation (12) while the factor c of the exponential terms depends on the initialization and the noise. If we initialize the parameters far from the origin, i.e. $\beta \gg 0$, the nonlinearity of fine-tuning dynamics would force the loss to converge faster. On the other hand, if the random mechanism perturbs the gradient more, i.e. σ increases, then the noise slows down the convergence. When we take limit $\sigma \rightarrow 0$ in Theorem 3.10 and 3.11, the Langevin diffusion degenerates to a gradient flow and the loss converges exponentially to zero as $t \rightarrow \infty$. This recovers known results from the non-private optimization literature [64].

There is still room for improvement in Theorem 3.11. The upper bound is loose in the sense that it does not incorporate γ , the pretraining quality. Nonetheless, we can develop new theoretical results based on this upper bound.

3.4 Linear probing vs. fine-tuning

The following result identifies a condition under which linear probing may work better than fine-tuning. Note that we cannot conclude that linear probing is definitively better than fine-tuning for our model, as both Theorem 3.10 and Theorem 3.11 are upper bounds. However, we observe empirically that the predictions that come from this condition appear to qualitatively hold.

Corollary 3.12

For simplicity, we assume that $X^T X = I_{d \times d}$. Suppose Assumption 3.3 and 3.4 hold. Then linear probing achieves a smaller loss upper bound in expectation if:

$$t \rightarrow \infty \text{ and } \gamma < \frac{\sigma^2}{c}((1 + d)\|X^T Y\| + d) - k\sigma^2. \quad (14)$$

The intuition of Corollary 3.12 is that a linear head works better given better pretrained features (i.e. smaller γ), a smaller size of the linear head, a larger noise scale, and enough running time. Otherwise, fine-tuning will eventually achieve a smaller loss than linear probing as $t \rightarrow \infty$.

3.5 First-linear-probing-then-finetuning

We next study the two-phase fine-tuning method of linear probing followed by full fine-tuning. We refer to this strategy as LP-FT, and find that it may work better in some settings than linear probing

or full fine-tuning alone. Linear probing first can accelerate fine-tuning by aligning the linear head. The following result provides a convergence bound for LP-FT when we linear-probe for time t_{lp} , and then fully fine-tune for time t .

Proposition 3.13 (Linear probing accelerates fine-tuning)

For simplicity, we assume that $\tilde{X}^T X = I_{d \times d}$. If Assumption 3.3 and 3.4 hold, and we run linear probing for time t_{lp} and then fine-tuning (Equation (10)) for time t , then the loss is upper bounded by:

$$\mathbb{E}[\mathcal{L}(t)] \leq \mathbb{E}[\mathcal{L}_{lp}]e^{-ct} + L^\square(1 - e^{-ct}) \quad (15)$$

where \mathcal{L}_{lp} is the expected loss after linear probing. The coefficient $c = \mathbb{E}[\lambda_{\max}(D)] > 0$ increases as t_{lp} increases when we run linear probing in a finite time interval $t_{lp} \in \left(0, \ln \left[3 + \frac{k(\sigma^2 - \beta)}{\|B_0 X^T Y\|^2}\right]\right)$.

Corollary 3.14

For simplicity, we assume that $X^T X = I_{d \times d}$. Suppose Assumption 3.3 and 3.4 hold. Then the two-phase method, first-linear-probing-then-finetuning (LP-FT), could achieve a tighter loss upper bound than linear probing or fine-tuning in expectation if we first run linear probing for $t_{lp} \in \left(0, \ln \left[3 + \frac{k(\sigma^2 - \beta)}{\|B_0 X^T Y\|^2}\right]\right)$.

By Corollary 3.14, we predict that: when we fix other hyperparameters (e.g. the total training time T), the performance of LP-FT depends on the noise scale σ . If σ is large enough such that $T < \ln \left[3 + \frac{k(\sigma^2 - \beta)}{\|B_0 X^T Y\|^2}\right]$, then LP is the best; if σ is small enough such that $\ln \left[3 + \frac{k(\sigma^2 - \beta)}{\|B_0 X^T Y\|^2}\right] \leq 0$, then FT is the best; LP-FT could achieve the best performance when the noise scale is in a proper interval $\sigma^2 \in \left(\beta - 2\frac{\|B_0 X^T Y\|^2}{k}, \beta + (e^T - 3)\frac{\|B_0 X^T Y\|^2}{k}\right)$. We qualitatively verify this prediction in our experiments in Section 4.3.

4 Experiments

4.1 Experimental settings

We run experiments on five deep learning models and four transfer learning benchmarks to verify if our theoretical prediction, the existence of concave utility curves, generalizes to deep neural networks and real datasets. Each experimental setting comprises: (1) a model architecture, (2) a (larger) dataset for public pretraining, and (3) a (smaller) dataset as the private data for fine-tuning. The benchmarks we use are:

- ImageNet-1K→CIFAR-10. ImageNet-1K is a large-scale dataset. We initialize pretrained features of ResNet-50 from MoCo-v2 [21] and MoCo-v3 [22], trained on ImageNet-1K [73] without privacy. We then privately fine-tune the ResNet-50 on CIFAR-10.
- ImageNet-1K→STL-10. We pretrain a DeiT model on ImageNet then pretrain a Mini-DeiT-Ti model with weight distillation from the DeiT model [78, 94]. After that, we privately fine-tune the Mini-DeiT-Ti model on STL-10 [26] for 20 epochs.
- CIFAR-10→STL-10. We pretrain the feature extractor on CIFAR-10 [51] using stochastic gradient descent without privacy mechanisms. Then we finetune the pretrained features and a randomly initialized linear head on STL-10. This benchmark has been studied in the context of domain adaptation [35, 52]. The training subset of STL-10 only contains 500 images. To align with the small scale fine-tuning data, we run the experiments with smaller and data-efficient models: MobileNet-v3 and ResNet-18.
- RandP→CIFAR-10. To reproduce the results of Tang et al. [76] and verify the general existence of concave utility curves, we also consider a slightly non-standard pretraining protocol. We pretrain a wide residual network (WRN) [92] on synthetic images generated by random diffusion processes. We follow the settings in [76].

For each fine-tuning method, {linear probing (LP), full fine-tuning (FT), first-linear-probing-then-full-finetuning (LP-FT)}, we use a batch size of 64 and sweep over 3 learning rates {0.1, 0.05, 0.025}. We fine-tune for $e = 10$ epochs in total, employ early stopping, and select the optimal learning rate based on the accuracy of the in-distribution validation. To demonstrate utility curves on LP-FT (e.g.,

Model	# of param.	benchmark	σ	LP	LP-FT	FT
MobileNet-v3	1.52×10^6	CIFAR-10→STL-10	0.0	71.12 (0.31)	71.30 (0.11)	77.02 (0.31)
MobileNet-v3	1.52×10^6	CIFAR-10→STL-10	0.5	69.31 (0.03)	71.96 (0.11)	61.97 (0.14)
MobileNet-v3	1.52×10^6	CIFAR-10→STL-10	1.0	69.25 (0.05)	70.98 (0.14)	60.02 (0.21)
MobileNet-v3	1.52×10^6	CIFAR-10→STL-10	5.0	67.09 (0.18)	65.59 (0.18)	43.64 (0.17)
Mini-DeiT-Ti	2.89×10^6	ImageNet-1K→STL-10	0.0	95.74 (0.04)	96.82 (0.08)	96.17 (0.08)
Mini-DeiT-Ti	2.89×10^6	ImageNet-1K→STL-10	0.1	95.29 (0.05)	96.09 (0.01)	94.52 (0.16)
Mini-DeiT-Ti	2.89×10^6	ImageNet-1K→STL-10	5.0	93.17 (0.09)	91.52 (0.33)	53.94 (1.65)
ResNet-18	1.11×10^7	CIFAR-10→STL-10	0.0	67.92 (0.22)	67.71 (0.26)	71.45 (0.36)
ResNet-18	1.11×10^7	CIFAR-10→STL-10	0.5	63.92 (0.04)	64.85 (0.11)	52.17 (0.11)
ResNet-18	1.11×10^7	CIFAR-10→STL-10	1.0	63.91 (0.02)	64.68 (0.26)	51.73 (0.15)
ResNet-18	1.11×10^7	CIFAR-10→STL-10	3.0	63.52 (0.07)	62.11 (0.69)	47.87 (0.82)
ResNet-50	2.56×10^7	ImageNet-1K→CIFAR-10	0.0	82.35 (0.07)	95.54 (0.06)	96.82 (0.01)
ResNet-50	2.56×10^7	ImageNet-1K→CIFAR-10	0.1	61.31 (0.55)	69.55 (0.44)	69.93 (0.24)
ResNet-50	2.56×10^7	ImageNet-1K→CIFAR-10	0.3	61.06 (0.27)	66.13 (1.01)	53.30 (0.36)
ResNet-50	2.56×10^7	ImageNet-1K→CIFAR-10	0.5	61.12 (0.54)	60.81 (0.72)	40.70 (0.31)
ResNet-50	2.56×10^7	ImageNet-1K→CIFAR-10	1.0	60.36 (0.49)	59.83 (0.74)	30.92 (1.12)
WRN-16-4	4.37×10^7	RandP→CIFAR-10	9.3	61.2 (-)	72.32 (-)	69.1 (-)

Table 1: Selected results on four DP fine-tuning benchmarks and five model architectures. As suggested by Corollary 3.14, as the noise scale σ increases, the best fine-tuning strategy changes from full fine-tuning (FT) (small σ , low privacy regime) to linear-probing-then-full-finetuning (LP-FT), to linear probing (LP) (large σ , high privacy regime). We sort the rows by the number of parameters of each model and the noise scale in an ascending order. For each experiment setting, we report average test accuracies with standard errors.

Figure 2), we vary the number of epochs of linear probing from $e_{LP} = 0$ to $e_{LP} = 10$; all remaining epochs are allocated to full fine-tuning, i.e., $e_{FT} = 10 - e_{LP}$. Note that full fine-tuning corresponds to $e_{LP} = 0$ (the leftmost point of our plots), and linear probing corresponds to $e_{LP} = 10$. For experiments that simply compare LP, FT, and LP-FT (Table 1), we implement the LP-FT baseline by running $e_{LP} = 5$ epochs of linear probing and $e_{FT} = 5$ epochs of full fine-tuning. For all private optimization steps, we apply DP-SGD (a variant of DP-GD that operates over minibatches in each iteration) as specified by Abadi et al. [1] (i.e., we do not vary the noise by layer). This was done to observe whether our predictions hold under the most common usage of private optimization with DP-SGD. The test accuracy of each setting is an average over 3 random seeds.

4.2 Existence of non-monotonic utility curves

In this part, we empirically characterize the utility curve in more details.

DP settings. For the ImageNet-1K→CIFAR-10 benchmark, we change the epochs allocated to linear probing (see Figure 2). As one increases the fraction of rounds used for linear probing, test accuracy increases up to a point, then decreases. This kind of utility curves also exist in the RandP→CIFAR-10 benchmark with $\sigma = 9.3$ [76].

Non-DP settings. We fine-tune the pretrained ResNet-50 on CIFAR-10 without privacy mechanisms. The utility curves are monotonically decreasing as we increase the number of epochs allocated to linear probing (Figure 2).

4.3 Examining the theoretical predictions

One prediction from our theory (Corollary 3.14) is that there exist two thresholds $0 < c_1 < c_2$ for the noise scale σ such that we can qualitatively rank the expected empirical losses $\mathbb{E}[\mathcal{L}_{lp}], \mathbb{E}[\mathcal{L}_{ft}], \mathbb{E}[\mathcal{L}_{lp-ft}]$ of LP, FT, and LP-FT. In this comparison, our LP-FT baseline consists of half linear probing epochs, and half full fine-tuning epochs.

- if $\sigma < c_1$, then $\mathbb{E}[\mathcal{L}_{ft}] < \mathbb{E}[\mathcal{L}_{lp-ft}] < \mathbb{E}[\mathcal{L}_{lp}]$, i.e. full fine-tuning is the best choice;

- if $\sigma \in (c_1, c_2)$, then $\mathbb{E}[\mathcal{L}_{lp-ft}] < \min\{\mathbb{E}[\mathcal{L}_{lp}], \mathbb{E}[\mathcal{L}_{ft}]\}$, i.e. first-linear-probing-then-full-finetuning is the best choice;
- if $\sigma > c_2$, then $\mathbb{E}[\mathcal{L}_{lp}] < \mathbb{E}[\mathcal{L}_{lp-ft}] < \mathbb{E}[\mathcal{L}_{ft}]$, i.e. linear probing is the best choice.

To qualitatively test this prediction, we sweep over different noise scales σ and fix other hyperparameters in each benchmark and model architecture (see Table 1). As expected, among the three fine-tuning methods, FT almost always does the best under small noise scales (including the non-private setting where $\sigma = 0$), LP-FT does the best under moderate noise scales, and LP does the best under large noise scales. This trend holds across all four benchmarks we evaluated. The final row for WRN-16-4 was conducted only to reproduce the results of [76].

5 Conclusion

Our work explores the impact of differentially-private (DP) fine-tuning strategies on model optimization in machine learning pipelines. We observe that the traditional approach of full fine-tuning, where all model parameters are updated, does not always yield the best test accuracy, even for in-distribution data. Instead, we explore a sequential fine-tuning strategy that combines linear probing and full fine-tuning (LP-FT), and empirically demonstrate its superiority over individual approaches.

Through theoretical analysis on a two-layer linear network regression task, we provide evidence that DP linear probing can outperform DP full fine-tuning, particularly when privacy budgets are limited. For the two-phase sequential approach (LP-FT), our theoretical results reveal a utility curve, suggesting LP-FT can outperform either of linear probing or full fine-tuning alone, even when pre-trained features are highly effective. Our experiments across various fine-tuning benchmarks and model architectures consistently demonstrate the existence of utility curves, reinforcing the validity of our theoretical model.

A limitation of our analysis is that we do not have lower bounds on the convergence rates for linear probing or full fine-tuning. This prevents us from being able to conclusively state that one fine-tuning method is better than the other in any regime. Developing a lower bound for these convergence rates is an interesting question for future work.

References

- [1] Martin Abadi, Andy Chu, Ian Goodfellow, H. Brendan McMahan, Ilya Mironov, Kunal Talwar, and Li Zhang. Deep learning with differential privacy. In *Proceedings of the 2016 ACM SIGSAC Conference on Computer and Communications Security, CCS '16*, page 308–318, New York, NY, USA, 2016. Association for Computing Machinery. ISBN 9781450341394. doi: 10.1145/2976749.2978318. URL <https://doi.org/10.1145/2976749.2978318>.
- [2] Zeyuan Allen-Zhu, Yuanzhi Li, and Zhao Song. A convergence theory for deep learning via overparameterization. In Kamalika Chaudhuri and Ruslan Salakhutdinov, editors, *Proceedings of the 36th International Conference on Machine Learning*, volume 97 of *Proceedings of Machine Learning Research*, pages 242–252. PMLR, 09–15 Jun 2019. URL <https://proceedings.mlr.press/v97/allen-zhu19a.html>.
- [3] Sanjeev Arora, Nadav Cohen, and Elad Hazan. On the optimization of deep networks: Implicit acceleration by overparameterization. In Jennifer Dy and Andreas Krause, editors, *Proceedings of the 35th International Conference on Machine Learning*, volume 80 of *Proceedings of Machine Learning Research*, pages 244–253. PMLR, 10–15 Jul 2018. URL <https://proceedings.mlr.press/v80/arora18a.html>.
- [4] Sanjeev Arora, Nadav Cohen, Noah Golowich, and Wei Hu. A convergence analysis of gradient descent for deep linear neural networks. In *International Conference on Learning Representations*, 2019. URL <https://openreview.net/forum?id=SkMQg3C5K7>.
- [5] Sanjeev Arora, Simon Du, Wei Hu, Zhiyuan Li, and Ruosong Wang. Fine-grained analysis of optimization and generalization for overparameterized two-layer neural networks. In Kamalika Chaudhuri and Ruslan Salakhutdinov, editors, *Proceedings of the 36th International Conference on Machine Learning*, volume 97 of *Proceedings of Machine Learning Research*, pages 322–332. PMLR, 09–15 Jun 2019. URL <https://proceedings.mlr.press/v97/arora19a.html>.

- [6] Hilal Asi, Vitaly Feldman, Tomer Koren, and Kunal Talwar. Private stochastic convex optimization: Optimal rates in ℓ_1 geometry. In Marina Meila and Tong Zhang, editors, *Proceedings of the 38th International Conference on Machine Learning*, volume 139 of *Proceedings of Machine Learning Research*, pages 393–403. PMLR, 18–24 Jul 2021. URL <https://proceedings.mlr.press/v139/asi21b.html>.
- [7] Krishna Balasubramanian, Sinho Chewi, Murat A Erdogdu, Adil Salim, and Shunshi Zhang. Towards a theory of non-log-concave sampling: first-order stationarity guarantees for langevin monte carlo. In Po-Ling Loh and Maxim Raginsky, editors, *Proceedings of Thirty Fifth Conference on Learning Theory*, volume 178 of *Proceedings of Machine Learning Research*, pages 2896–2923. PMLR, 02–05 Jul 2022. URL <https://proceedings.mlr.press/v178/balasubramanian22a.html>.
- [8] Rina Foygel Barber and John C. Duchi. Privacy and statistical risk: Formalisms and minimax bounds. *ArXiv*, abs/1412.4451, 2014. URL <https://api.semanticscholar.org/CorpusID:2455782>.
- [9] Raef Bassily, Adam Smith, and Abhradeep Thakurta. Private empirical risk minimization: Efficient algorithms and tight error bounds. In *2014 IEEE 55th Annual Symposium on Foundations of Computer Science*, pages 464–473, 2014. doi: 10.1109/FOCS.2014.56.
- [10] Raef Bassily, Vitaly Feldman, Kunal Talwar, and Abhradeep Guha Thakurta. Private stochastic convex optimization with optimal rates. In H. Wallach, H. Larochelle, A. Beygelzimer, F. d’Alché-Buc, E. Fox, and R. Garnett, editors, *Advances in Neural Information Processing Systems*, volume 32. Curran Associates, Inc., 2019. URL https://proceedings.neurips.cc/paper_files/paper/2019/file/3bd8fdb090f1f5eb66a00c84dbc5ad51-Paper.pdf.
- [11] Raef Bassily, Cristóbal Guzmán, and Michael Menart. Differentially private stochastic optimization: New results in convex and non-convex settings. In M. Ranzato, A. Beygelzimer, Y. Dauphin, P.S. Liang, and J. Wortman Vaughan, editors, *Advances in Neural Information Processing Systems*, volume 34, pages 9317–9329. Curran Associates, Inc., 2021. URL https://proceedings.neurips.cc/paper_files/paper/2021/file/4ddb5b8d603f88e9de689f3230234b47-Paper.pdf.
- [12] Raef Bassily, Mehryar Mohri, and Ananda Theertha Suresh. Differentially private learning with margin guarantees. In S. Koyejo, S. Mohamed, A. Agarwal, D. Belgrave, K. Cho, and A. Oh, editors, *Advances in Neural Information Processing Systems*, volume 35, pages 32127–32141. Curran Associates, Inc., 2022.
- [13] Alex Bie, Gautam Kamath, and Vikrant Singhal. Private estimation with public data. In Alice H. Oh, Alekh Agarwal, Danielle Belgrave, and Kyunghyun Cho, editors, *Advances in Neural Information Processing Systems*, 2022. URL https://openreview.net/forum?id=YpyGV_i8Z_J.
- [14] Zhiqi Bu, Yu-Xiang Wang, Sheng Zha, and George Karypis. Differentially private optimization on large model at small cost. *arXiv preprint arXiv:2210.00038*, 2022.
- [15] Zhiqi Bu, Yu-Xiang Wang, Sheng Zha, and George Karypis. Differentially private bias-term only fine-tuning of foundation models. *arXiv preprint arXiv:2210.00036*, 2022.
- [16] Zhiqi Bu, Hua Wang, Zongyu Dai, and Qi Long. On the convergence and calibration of deep learning with differential privacy. *Transactions on Machine Learning Research*, 2023. ISSN 2835-8856. URL <https://openreview.net/forum?id=KOCAGgjYS1>.
- [17] Sébastien Bubeck, Ronen Eldan, and Joseph Lehec. Sampling from a log-concave distribution with projected langevin monte carlo. *Discrete & Computational Geometry*, 59:757 – 783, 2015. URL <https://api.semanticscholar.org/CorpusID:16530097>.
- [18] Sébastien Bubeck, Ronen Eldan, and Joseph Lehec. Sampling from a log-concave distribution with projected langevin monte carlo. *Discrete Comput. Geom.*, 59(4):757–783, jun 2018. ISSN 0179-5376. doi: 10.1007/s00454-018-9992-1. URL <https://doi.org/10.1007/s00454-018-9992-1>.

- [19] Yuan Cao and Quanquan Gu. Generalization bounds of stochastic gradient descent for wide and deep neural networks. In H. Wallach, H. Larochelle, A. Beygelzimer, F. d'Alché-Buc, E. Fox, and R. Garnett, editors, *Advances in Neural Information Processing Systems*, volume 32. Curran Associates, Inc., 2019. URL https://proceedings.neurips.cc/paper_files/paper/2019/file/cf9dc5e4e194fc21f397b4cac9cc3ae9-Paper.pdf.
- [20] Xiangyi Chen, Zhiwei Steven Wu, and Mingyi Hong. Understanding gradient clipping in private sgd: A geometric perspective. In *Proceedings of the 34th International Conference on Neural Information Processing Systems, NIPS'20*, Red Hook, NY, USA, 2020. Curran Associates Inc. ISBN 9781713829546.
- [21] Xinlei Chen, Haoqi Fan, Ross Girshick, and Kaiming He. Improved baselines with momentum contrastive learning. *arXiv preprint arXiv:2003.04297*, 2020.
- [22] Xinlei Chen*, Saining Xie*, and Kaiming He. An empirical study of training self-supervised vision transformers. *arXiv preprint arXiv:2104.02057*, 2021.
- [23] Xiang Cheng, Niladri S. Chatterji, Yasin Abbasi-Yadkori, Peter L. Bartlett, and Michael I. Jordan. Sharp convergence rates for langevin dynamics in the nonconvex setting. *ArXiv*, abs/1805.01648, 2018. URL <https://api.semanticscholar.org/CorpusID:21129457>.
- [24] Sinho Chewi, Murat A Erdogdu, Mufan Li, Ruoqi Shen, and Shunshi Zhang. Analysis of langevin monte carlo from poincare to log-sobolev. In Po-Ling Loh and Maxim Raginsky, editors, *Proceedings of Thirty Fifth Conference on Learning Theory*, volume 178 of *Proceedings of Machine Learning Research*, pages 1–2. PMLR, 02–05 Jul 2022. URL <https://proceedings.mlr.press/v178/chewi22a.html>.
- [25] Rishav Chourasia, Jiayuan Ye, and Reza Shokri. Differential privacy dynamics of langevin diffusion and noisy gradient descent. In M. Ranzato, A. Beygelzimer, Y. Dauphin, P.S. Liang, and J. Wortman Vaughan, editors, *Advances in Neural Information Processing Systems*, volume 34, pages 14771–14781. Curran Associates, Inc., 2021. URL https://proceedings.neurips.cc/paper_files/paper/2021/file/7c6c1a7bfde175bed616b39247ccace1-Paper.pdf.
- [26] Adam Coates, Andrew Ng, and Honglak Lee. An analysis of single-layer networks in unsupervised feature learning. In Geoffrey Gordon, David Dunson, and Miroslav Dudík, editors, *Proceedings of the Fourteenth International Conference on Artificial Intelligence and Statistics*, volume 15 of *Proceedings of Machine Learning Research*, pages 215–223, Fort Lauderdale, FL, USA, 11–13 Apr 2011. PMLR. URL <https://proceedings.mlr.press/v15/coates11a.html>.
- [27] Rachel Cummings, Damien Desfontaines, David Evans, Roxana Geambasu, Matthew Jagielski, Yangsibo Huang, Peter Kairouz, Gautam Kamath, Sewoong Oh, Olga Ohrimenko, Nicolas Papernot, Ryan Rogers, Milan Shen, Shuang Song, Weijie Su, Andreas Terzis, Abhradeep Thakurta, Sergei Vassilvitskii, Yu-Xiang Wang, Li Xiong, Sergey Yekhanin, Da Yu, Huanyu Zhang, and Wanrong Zhang. Challenges towards the next frontier in privacy, 2023.
- [28] Soham De, Leonard Berrada, Jamie Hayes, Samuel L Smith, and Borja Balle. Unlocking High-Accuracy Differentially Private Image Classification through Scale. *arXiv preprint arXiv:2204.13650*, 2022.
- [29] Alexey Dosovitskiy, Lucas Beyer, Alexander Kolesnikov, Dirk Weissenborn, Xiaohua Zhai, Thomas Unterthiner, Mostafa Dehghani, Matthias Minderer, Georg Heigold, Sylvain Gelly, Jakob Uszkoreit, and Neil Houlsby. An image is worth 16x16 words: Transformers for image recognition at scale. In *International Conference on Learning Representations*, 2021. URL <https://openreview.net/forum?id=YicbFdNTTy>.
- [30] Simon S Du, Wei Hu, and Jason D Lee. Algorithmic regularization in learning deep homogeneous models: Layers are automatically balanced. In S. Bengio, H. Wallach, H. Larochelle, K. Grauman, N. Cesa-Bianchi, and R. Garnett, editors, *Advances in Neural Information Processing Systems*, volume 31. Curran Associates, Inc., 2018. URL https://proceedings.neurips.cc/paper_files/paper/2018/file/fe131d7f5a6b38b23cc967316c13dae2-Paper.pdf.

- [31] Cynthia Dwork and Aaron Roth. The algorithmic foundations of differential privacy. *Found. Trends Theor. Comput. Sci.*, 9(3–4):211–407, aug 2014. ISSN 1551-305X. doi: 10.1561/04000000042. URL <https://doi.org/10.1561/04000000042>.
- [32] Omer Elkabetz and Nadav Cohen. Continuous vs. discrete optimization of deep neural networks. In A. Beygelzimer, Y. Dauphin, P. Liang, and J. Wortman Vaughan, editors, *Advances in Neural Information Processing Systems*, 2021. URL <https://openreview.net/forum?id=iX0TSH45e0d>.
- [33] Murat A Erdogdu and Rasa Hosseinzadeh. On the convergence of langevin monte carlo: The interplay between tail growth and smoothness. In Mikhail Belkin and Samory Kpotufe, editors, *Proceedings of Thirty Fourth Conference on Learning Theory*, volume 134 of *Proceedings of Machine Learning Research*, pages 1776–1822. PMLR, 15–19 Aug 2021. URL <https://proceedings.mlr.press/v134/erdogdu21a.html>.
- [34] Murat A. Erdogdu, Rasa Hosseinzadeh, and Shunshi Zhang. Convergence of langevin monte carlo in chi-squared and rényi divergence. In Gustau Camps-Valls, Francisco J. R. Ruiz, and Isabel Valera, editors, *Proceedings of The 25th International Conference on Artificial Intelligence and Statistics*, volume 151 of *Proceedings of Machine Learning Research*, pages 8151–8175. PMLR, 28–30 Mar 2022. URL <https://proceedings.mlr.press/v151/erdogdu22a.html>.
- [35] Geoff French, Michal Mackiewicz, and Mark Fisher. Self-ensembling for visual domain adaptation. In *International Conference on Learning Representations*, 2018. URL <https://openreview.net/forum?id=rkpoTaxA->.
- [36] Arun Ganesh, Mahdi Haghifam, Milad Nasr, Sewoong Oh, Thomas Steinke, Om Thakkar, Abhradeep Guha Thakurta, and Lun Wang. Why is public pretraining necessary for private model training? In Andreas Krause, Emma Brunskill, Kyunghyun Cho, Barbara Engelhardt, Sivan Sabato, and Jonathan Scarlett, editors, *Proceedings of the 40th International Conference on Machine Learning*, volume 202 of *Proceedings of Machine Learning Research*, pages 10611–10627. PMLR, 23–29 Jul 2023. URL <https://proceedings.mlr.press/v202/ganesh23a.html>.
- [37] Arun Ganesh, Abhradeep Thakurta, and Jalaj Upadhyay. Universality of langevin diffusion for private optimization, with applications to sampling from rashomon sets. In Gergely Neu and Lorenzo Rosasco, editors, *Proceedings of Thirty Sixth Conference on Learning Theory*, volume 195 of *Proceedings of Machine Learning Research*, pages 1730–1773. PMLR, 12–15 Jul 2023. URL <https://proceedings.mlr.press/v195/ganesh23a.html>.
- [38] Sachin Goyal, Ananya Kumar, Sankalp Garg, Zico Kolter, and Aditi Raghunathan. Finetune like you pretrain: Improved finetuning of zero-shot vision models. In *Proceedings of the IEEE/CVF Conference on Computer Vision and Pattern Recognition (CVPR)*, pages 19338–19347, June 2023.
- [39] Seokhyeon Ha, Sunbeom Jung, and Jungwoo Lee. Domain-aware fine-tuning: Enhancing neural network adaptability, 2024.
- [40] Kaiming He, Xiangyu Zhang, Shaoqing Ren, and Jian Sun. Delving deep into rectifiers: Surpassing human-level performance on imagenet classification. In *2015 IEEE International Conference on Computer Vision (ICCV)*, pages 1026–1034, 2015. doi: 10.1109/ICCV.2015.123.
- [41] Kaiming He, Xiangyu Zhang, Shaoqing Ren, and Jian Sun. Deep residual learning for image recognition. In *2016 IEEE Conference on Computer Vision and Pattern Recognition (CVPR)*, pages 770–778, 2016. doi: 10.1109/CVPR.2016.90.
- [42] Kaiming He, Haoqi Fan, Yuxin Wu, Saining Xie, and Ross Girshick. Momentum contrast for unsupervised visual representation learning. In *Proceedings of the IEEE/CVF Conference on Computer Vision and Pattern Recognition (CVPR)*, June 2020.
- [43] Shlomo Hoory, Amir Feder, Avichai Tendler, Alon Cohen, Sofia Erell, Itay Laish, Hootan Nakhost, Uri Stemmer, Ayelet Benjamini, Avinatan Hassidim, and Yossi Matias. Learning

- and evaluating a differentially private pre-trained language model. In Oluwaseyi Feyisetan, Sepideh Ghanavati, Shervin Malmasi, and Patricia Thaine, editors, *Proceedings of the Third Workshop on Privacy in Natural Language Processing*, pages 21–29, Online, June 2021. Association for Computational Linguistics. doi: 10.18653/v1/2021.privatenlp-1.3. URL <https://aclanthology.org/2021.privatenlp-1.3>.
- [44] Charlie Hou, Hongyuan Zhan, Akshat Shrivastava, Sid Wang, Aleksandr Livshits, Giulia Fanti, and Daniel Lazar. Privately customizing prefinetuning to better match user data in federated learning. In *ICLR 2023 Workshop on Pitfalls of limited data and computation for Trustworthy ML*, 2023. URL https://openreview.net/forum?id=0Wb_1ZuEwyI.
- [45] A. Howard, M. Sandler, B. Chen, W. Wang, L. Chen, M. Tan, G. Chu, V. Vasudevan, Y. Zhu, R. Pang, H. Adam, and Q. Le. Searching for mobilenetv3. In *2019 IEEE/CVF International Conference on Computer Vision (ICCV)*, pages 1314–1324, Los Alamitos, CA, USA, nov 2019. IEEE Computer Society. doi: 10.1109/ICCV.2019.00140. URL <https://doi.ieeecomputersociety.org/10.1109/ICCV.2019.00140>.
- [46] Andong Hua, Jindong Gu, Zhiyu Xue, Nicholas Carlini, Eric Wong, and Yao Qin. Initialization matters for adversarial transfer learning, 2023.
- [47] Chao Huang, Geng Tian, and Ming Tang. When minibatch sgd meets splitfed learning: convergence analysis and performance evaluation, 2023.
- [48] Tim Johnston and Sotirios Sabanis. Convergence of the unadjusted langevin algorithm for discontinuous gradients, 2023.
- [49] Polina Kirichenko, Pavel Izmailov, and Andrew Gordon Wilson. Last layer re-training is sufficient for robustness to spurious correlations. In *The Eleventh International Conference on Learning Representations*, 2023. URL <https://openreview.net/forum?id=Zb6c8A-Fghk>.
- [50] Simon Kornblith, Jonathon Shlens, and Quoc V. Le. Do better imagenet models transfer better? In *Proceedings of the IEEE/CVF Conference on Computer Vision and Pattern Recognition (CVPR)*, June 2019.
- [51] Alex Krizhevsky. Learning multiple layers of features from tiny images. Technical report, Canadian Institute for Advanced Research, 2009.
- [52] Ananya Kumar, Aditi Raghunathan, Robbie Matthew Jones, Tengyu Ma, and Percy Liang. Fine-tuning can distort pretrained features and underperform out-of-distribution. In *International Conference on Learning Representations*, 2022. URL <https://openreview.net/forum?id=UYneFzXSJWh>.
- [53] Yann LeCun, Bernhard Boser, John Denker, Donnie Henderson, R. Howard, Wayne Hubbard, and Lawrence Jackel. Handwritten digit recognition with a back-propagation network. In D. Touretzky, editor, *Advances in Neural Information Processing Systems*, volume 2. Morgan-Kaufmann, 1989. URL https://proceedings.neurips.cc/paper_files/paper/1989/file/53c3bce66e43be4f209556518c2fcb54-Paper.pdf.
- [54] Don S. Lemons and Anthony Gythiel. Paul Langevin’s 1908 paper “On the Theory of Brownian Motion” [“Sur la théorie du mouvement brownien,” C. R. Acad. Sci. (Paris) 146, 530–533 (1908)]. *American Journal of Physics*, 65(11):1079–1081, 11 1997. ISSN 0002-9505. doi: 10.1119/1.18725. URL <https://doi.org/10.1119/1.18725>.
- [55] Qianxiao Li, Cheng Tai, and Weinan E. Stochastic modified equations and dynamics of stochastic gradient algorithms i: Mathematical foundations. *Journal of Machine Learning Research*, 20(40):1–47, 2019. URL <http://jmlr.org/papers/v20/17-526.html>.
- [56] Tian Li, Manzil Zaheer, Sashank Reddi, and Virginia Smith. Private adaptive optimization with side information. In Kamalika Chaudhuri, Stefanie Jegelka, Le Song, Csaba Szepesvari, Gang Niu, and Sivan Sabato, editors, *Proceedings of the 39th International Conference on Machine Learning*, volume 162 of *Proceedings of Machine Learning Research*, pages 13086–13105. PMLR, 17–23 Jul 2022. URL <https://proceedings.mlr.press/v162/li22x.html>.

- [57] Tian Li, Manzil Zaheer, Ken Liu, Sashank J. Reddi, Hugh Brendan McMahan, and Virginia Smith. Differentially private adaptive optimization with delayed preconditioners. In *The Eleventh International Conference on Learning Representations*, 2023. URL <https://openreview.net/forum?id=j1zQGmQQ0X1>.
- [58] Xuechen Li, Daogao Liu, Tatsunori Hashimoto, Huseyin A Inan, Janardhan Kulkarni, YinTat Lee, and Abhradeep Guha Thakurta. When does differentially private learning not suffer in high dimensions? In Alice H. Oh, Alekh Agarwal, Danielle Belgrave, and Kyunghyun Cho, editors, *Advances in Neural Information Processing Systems*, 2022. URL <https://openreview.net/forum?id=FR--mkQu0dw>.
- [59] Xinyu Liu, Houwen Peng, Ningxin Zheng, Yuqing Yang, Han Hu, and Yixuan Yuan. Efficientvit: Memory efficient vision transformer with cascaded group attention. In *Proceedings of the IEEE/CVF Conference on Computer Vision and Pattern Recognition (CVPR)*, 2023.
- [60] Sibylle Marcotte, Rémi Gribonval, and Gabriel Peyré. Abide by the law and follow the flow: conservation laws for gradient flows. In *Thirty-seventh Conference on Neural Information Processing Systems*, 2023. URL <https://openreview.net/forum?id=kMueEV8Eyy>.
- [61] Amil Merchant, Elahe Rahimtoroghi, Ellie Pavlick, and Ian Tenney. What happens to BERT embeddings during fine-tuning? In Afra Alishahi, Yonatan Belinkov, Grzegorz Chrupała, Dieuwke Hupkes, Yuval Pinter, and Hassan Sajjad, editors, *Proceedings of the Third BlackboxNLP Workshop on Analyzing and Interpreting Neural Networks for NLP*, pages 33–44, Online, November 2020. Association for Computational Linguistics. doi: 10.18653/v1/2020.blackboxnlp-1.4. URL <https://aclanthology.org/2020.blackboxnlp-1.4>.
- [62] Hancheng Min, Salma Tarmoun, Rene Vidal, and Enrique Mallada. On the explicit role of initialization on the convergence and implicit bias of overparametrized linear networks. In Marina Meila and Tong Zhang, editors, *Proceedings of the 38th International Conference on Machine Learning*, volume 139 of *Proceedings of Machine Learning Research*, pages 7760–7768. PMLR, 18–24 Jul 2021. URL <https://proceedings.mlr.press/v139/min21c.html>.
- [63] Hancheng Min, René Vidal, and Enrique Mallada. Early neuron alignment in two-layer relu networks with small initialization. *ArXiv*, abs/2307.12851, 2023. URL <https://api.semanticscholar.org/CorpusID:260125817>.
- [64] Hancheng Min, Rene Vidal, and Enrique Mallada. On the convergence of gradient flow on multi-layer linear models. In Andreas Krause, Emma Brunskill, Kyunghyun Cho, Barbara Engelhardt, Sivan Sabato, and Jonathan Scarlett, editors, *Proceedings of the 40th International Conference on Machine Learning*, volume 202 of *Proceedings of Machine Learning Research*, pages 24850–24887. PMLR, 23–29 Jul 2023. URL <https://proceedings.mlr.press/v202/min23d.html>.
- [65] Taiki Miyagawa. Toward equation of motion for deep neural networks: Continuous-time gradient descent and discretization error analysis. In S. Koyejo, S. Mohamed, A. Agarwal, D. Belgrave, K. Cho, and A. Oh, editors, *Advances in Neural Information Processing Systems*, volume 35, pages 37778–37791. Curran Associates, Inc., 2022.
- [66] Wenlong Mou, Nicolas Flammarion, Martin J. Wainwright, and Peter L. Bartlett. Improved bounds for discretization of langevin diffusions: Near-optimal rates without convexity. *Bernoulli*, 28(3):1577–1601, 2022. doi: <https://doi.org/10.3150/21-BEJ1343>. URL <http://infoscience.epfl.ch/record/272852>.
- [67] Alireza Mousavi-Hosseini, Tyler K. Farghly, Ye He, Krishna Balasubramanian, and Murat A. Erdogdu. Towards a complete analysis of langevin monte carlo: Beyond poincaré inequality. In Gergely Neu and Lorenzo Rosasco, editors, *Proceedings of Thirty Sixth Conference on Learning Theory*, volume 195 of *Proceedings of Machine Learning Research*, pages 1–35. PMLR, 12–15 Jul 2023. URL <https://proceedings.mlr.press/v195/mousavi-hosseini23a.html>.
- [68] Behnam Neyshabur, Ryota Tomioka, and Nathan Srebro. In search of the real inductive bias: On the role of implicit regularization in deep learning. *CoRR*, abs/1412.6614, 2014. URL <https://api.semanticscholar.org/CorpusID:6021932>.

- [69] Dao Nguyen, Xin Dang, and Yixin Chen. Unadjusted langevin algorithm for non-convex weakly smooth potentials. *Communications in Mathematics and Statistics*, Dec 2023. ISSN 2194-671X. doi: 10.1007/s40304-023-00350-w. URL <https://doi.org/10.1007/s40304-023-00350-w>.
- [70] Sewoong Oh, Soumik Pal, Raghav Somani, and Raghavendra Tripathi. Gradient flows on graphons: Existence, convergence, continuity equations. *Journal of Theoretical Probability*, Jul 2023. ISSN 1572-9230. doi: 10.1007/s10959-023-01271-8. URL <https://doi.org/10.1007/s10959-023-01271-8>.
- [71] Houwen Peng, Hao Du, Hongyuan Yu, Qi Li, Jing Liao, and Jianlong Fu. Cream of the crop: Distilling prioritized paths for one-shot neural architecture search. *Advances in Neural Information Processing Systems*, 33, 2020.
- [72] Maxim Raginsky, Alexander Rakhlin, and Matus Telgarsky. Non-convex learning via stochastic gradient langevin dynamics: a nonasymptotic analysis. In Satyen Kale and Ohad Shamir, editors, *Proceedings of the 2017 Conference on Learning Theory*, volume 65 of *Proceedings of Machine Learning Research*, pages 1674–1703. PMLR, 07–10 Jul 2017. URL <https://proceedings.mlr.press/v65/raginsky17a.html>.
- [73] Olga Russakovsky, Jia Deng, Hao Su, Jonathan Krause, Sanjeev Satheesh, Sean Ma, Zhiheng Huang, Andrej Karpathy, Aditya Khosla, Michael Bernstein, Alexander C. Berg, and Li Fei-Fei. ImageNet Large Scale Visual Recognition Challenge. *International Journal of Computer Vision (IJCV)*, 115(3):211–252, 2015. doi: 10.1007/s11263-015-0816-y.
- [74] Tom Sander, Pierre Stock, and Alexandre Sablayrolles. Tan without a burn: scaling laws of dp-sgd. In *Proceedings of the 40th International Conference on Machine Learning, ICML'23*. JMLR.org, 2023.
- [75] Weijie Su, Stephen Boyd, and Emmanuel J. Candès. A differential equation for modeling nesterov’s accelerated gradient method: Theory and insights. *Journal of Machine Learning Research*, 17(153):1–43, 2016. URL <http://jmlr.org/papers/v17/15-084.html>.
- [76] Xinyu Tang, Ashwinee Panda, Vikash Sehwal, and Prateek Mittal. Differentially private image classification by learning priors from random processes. *CoRR*, 2023.
- [77] Salma Tarmoun, Guilherme Franca, Benjamin D Haeffele, and Rene Vidal. Understanding the dynamics of gradient flow in overparameterized linear models. In Marina Meila and Tong Zhang, editors, *Proceedings of the 38th International Conference on Machine Learning*, volume 139 of *Proceedings of Machine Learning Research*, pages 10153–10161. PMLR, 18–24 Jul 2021. URL <https://proceedings.mlr.press/v139/tarmoun21a.html>.
- [78] Hugo Touvron, Matthieu Cord, Matthijs Douze, Francisco Massa, Alexandre Sablayrolles, and Herve Jegou. Training data-efficient image transformers & distillation through attention. In Marina Meila and Tong Zhang, editors, *Proceedings of the 38th International Conference on Machine Learning*, volume 139 of *Proceedings of Machine Learning Research*, pages 10347–10357. PMLR, 18–24 Jul 2021. URL <https://proceedings.mlr.press/v139/touvron21a.html>.
- [79] Nilesh Tripuraneni, Michael Jordan, and Chi Jin. On the theory of transfer learning: The importance of task diversity. In H. Larochelle, M. Ranzato, R. Hadsell, M.F. Balcan, and H. Lin, editors, *Advances in Neural Information Processing Systems*, volume 33, pages 7852–7862. Curran Associates, Inc., 2020. URL https://proceedings.neurips.cc/paper_files/paper/2020/file/59587bfffec1c7846f3e34230141556ae-Paper.pdf.
- [80] Stephen Tu. On the exponential convergence of langevin diffusions: from deterministic to stochastic stability, 2022.
- [81] Heng Wang, Tan Yue, Xiang Ye, Zihang He, Bohan Li, and Yong Li. Revisit finetuning strategy for few-shot learning to transfer the emdeddings. In *The Eleventh International Conference on Learning Representations*, 2023. URL <https://openreview.net/forum?id=tXc-riXhmx>.

- [82] Tongzhou Wang and Phillip Isola. Understanding contrastive representation learning through alignment and uniformity on the hypersphere. In *Proceedings of the 37th International Conference on Machine Learning, ICML'20*. JMLR.org, 2020.
- [83] Xingyu Wang, Sewoong Oh, and Chang-Han Rhee. Eliminating sharp minima from SGD with truncated heavy-tailed noise. In *International Conference on Learning Representations, 2022*. URL <https://openreview.net/forum?id=B3Nde6lvab>.
- [84] Kan Wu, Jinnian Zhang, Houwen Peng, Mengchen Liu, Bin Xiao, Jianlong Fu, and Lu Yuan. Tinyvit: Fast pretraining distillation for small vision transformers. In *European conference on computer vision (ECCV), 2022*.
- [85] Pan Xu, Jinghui Chen, Difan Zou, and Quanquan Gu. Global convergence of langevin dynamics based algorithms for nonconvex optimization. In S. Bengio, H. Wallach, H. Larochelle, K. Grauman, N. Cesa-Bianchi, and R. Garnett, editors, *Advances in Neural Information Processing Systems*, volume 31. Curran Associates, Inc., 2018. URL https://proceedings.neurips.cc/paper_files/paper/2018/file/9c19a2aa1d84e04b0bd4bc888792bd1e-Paper.pdf.
- [86] Zhuoyi Yang, Ming Ding, Yanhui Guo, Qingsong Lv, and Jie Tang. Parameter-efficient tuning makes a good classification head, 2023.
- [87] Jiayuan Ye, Zhenyu Zhu, Fanghui Liu, Reza Shokri, and Volkan Cevher. Initialization matters: Privacy-utility analysis of overparameterized neural networks. In *Thirty-seventh Conference on Neural Information Processing Systems, 2023*. URL <https://openreview.net/forum?id=IKvxxmHjkl>.
- [88] Tian Ye and Simon Shaolei Du. Global convergence of gradient descent for asymmetric low-rank matrix factorization. In A. Beygelzimer, Y. Dauphin, P. Liang, and J. Wortman Vaughan, editors, *Advances in Neural Information Processing Systems*, 2021. URL <https://openreview.net/forum?id=sMIMAXqijq3>.
- [89] Ashkan Yousefpour, Igor Shilov, Alexandre Sablayrolles, Davide Testuggine, Karthik Prasad, Mani Malek, John Nguyen, Sayan Ghosh, Akash Bharadwaj, Jessica Zhao, Graham Cormode, and Ilya Mironov. Opacus: User-friendly differential privacy library in PyTorch. *arXiv preprint arXiv:2109.12298*, 2021.
- [90] Da Yu, Saurabh Naik, Arturs Backurs, Sivakanth Gopi, Huseyin A Inan, Gautam Kamath, Janardhan Kulkarni, Yin Tat Lee, Andre Manoel, Lukas Wutschitz, Sergey Yekhanin, and Huishuai Zhang. Differentially private fine-tuning of language models. In *International Conference on Learning Representations, 2022*. URL <https://openreview.net/forum?id=Q42f0dfjECO>.
- [91] Da Yu, Sivakanth Gopi, Janardhan Kulkarni, Zinan Lin, Saurabh Naik, Tomasz Lukasz Religa, Jian Yin, and Huishuai Zhang. Selective pre-training for private fine-tuning, 2023.
- [92] Sergey Zagoruyko and Nikos Komodakis. Wide Residual Networks. In *British Machine Vision Conference 2016*, York, France, January 2016. British Machine Vision Association. doi: 10.5244/C.30.87. URL <https://enpc.hal.science/hal-01832503>.
- [93] Xiaohua Zhai, Joan Puigcerver, Alexander Kolesnikov, Pierre Ruysen, Carlos Riquelme, Mario Lucic, Josip Djolonga, André Susano Pinto, Maxim Neumann, Alexey Dosovitskiy, Lucas Beyer, Olivier Bachem, Michael Tschannen, Marcin Michalski, Olivier Bousquet, Sylvain Gelly, and Neil Houlsby. A large-scale study of representation learning with the visual task adaptation benchmark. *arXiv: Computer Vision and Pattern Recognition*, 2019. URL <https://api.semanticscholar.org/CorpusID:214317405>.
- [94] Jinnian Zhang, Houwen Peng, Kan Wu, Mengchen Liu, Bin Xiao, Jianlong Fu, and Lu Yuan. Minivit: Compressing vision transformers with weight multiplexing. In *2022 IEEE/CVF Conference on Computer Vision and Pattern Recognition (CVPR)*, pages 12135–12144, 2022. doi: 10.1109/CVPR52688.2022.01183.
- [95] Meng Zhang, Ermin Wei, Randall Berry, and Jianwei Huang. Age-dependent differential privacy. *IEEE Transactions on Information Theory*, 70(2):1300–1319, 2024. doi: 10.1109/TIT.2023.3340147.

- [96] Shunshi Zhang, Sinho Chewi, Mufan Li, Krishna Balasubramanian, and Murat A. Erdogdu. Improved discretization analysis for underdamped langevin monte carlo. In Gergely Neu and Lorenzo Rosasco, editors, *Proceedings of Thirty Sixth Conference on Learning Theory*, volume 195 of *Proceedings of Machine Learning Research*, pages 36–71. PMLR, 12–15 Jul 2023. URL <https://proceedings.mlr.press/v195/zhang23a.html>.

A Proofs

A.1 Itô's formula and its consequences

Theorem A.1 (Itô's formula)

Let X_t be a \mathbb{R}^n -valued Itô process satisfying the stochastic differential equation $\partial X_t = A_1(t, X_t)\partial t + A_2(t, X_t)\partial W_t$ with $A_1(t, X_t)$ being \mathbb{R}^n -valued, $A_2(t, X_t)$ being $M_{m,n}(\mathbb{R})$ -valued, and W_t being a standard n -dimensional brownian motion. Let $f : [0, \infty) \times \mathbb{R}^n \rightarrow \mathbb{R}$ be a function with continuous partial derivatives. Then $Y_t := f(t, X_t)$ is also an Itô process, and its stochastic differential equation is

$$\partial Y_t = \frac{\partial f(t, X_t)}{\partial t} \partial t + \langle \nabla f(t, X_t), A_1(t, X_t) \partial t + A_2(t, X_t) \partial W_t \rangle + \frac{1}{2} \langle A_2(t, X_t) \partial W_t, H_f A_2(t, X_t) \partial W_t \rangle \quad (16)$$

where H_f is the Hessian matrix of f over X_t defined as $(H_f)_{ij} = \frac{\partial^2 f}{\partial (X_t)_i \partial (X_t)_j}$ and $(X_t)_i$ denotes the i -th entry of random vector X_t .

Corollary A.2 (Loss dynamics during linear probing)

During linear probing (Equation (4)), the stochastic differential equation describing the loss dynamics is

$$\partial \mathcal{L}_{\text{lp}} = -(B_0^T v - X^T Y)^T B_0^T B_0 (B_0^T v - X^T Y) \partial t + \sqrt{2\sigma^2} (B_0^T v - X^T Y)^T B_0^T \partial W_t + k\sigma^2 \partial t. \quad (17)$$

Proof of Corollary A.2. By Itô's formula (Equation (A.1)), the loss dynamics is

$$\partial \mathcal{L}_{\text{lp}} = \partial \frac{1}{2} \|X B_0^T v - Y\|^2 \quad (18)$$

$$= (X B_0^T v - Y)^T X B_0^T \partial v + \frac{1}{2} (\partial v)^T B_0 X^T X B_0^T (\partial v) \quad (19)$$

$$= (X B_0^T v - Y)^T X B_0^T \partial v + \frac{1}{2} (\partial v)^T (\partial v) \quad (20)$$

$$= (X B_0^T v - Y)^T X B_0^T [-B_0 X^T (X B_0^T v - Y) \partial t + \sqrt{2\sigma^2} \partial W_t] + k\sigma^2 \partial t \quad (21)$$

$$= (B_0^T v - X^T Y)^T B_0^T [-B_0 (B_0^T v - X^T Y) \partial t + \sqrt{2\sigma^2} \partial W_t] + k\sigma^2 \partial t \quad (22)$$

$$= -(B_0^T v - X^T Y)^T B_0^T B_0 (B_0^T v - X^T Y) \partial t + \sqrt{2\sigma^2} (B_0^T v - X^T Y)^T B_0^T \partial W_t + k\sigma^2 \partial t \quad (23)$$

□

Corollary A.3 (Loss dynamics during fine-tuning)

During fine-tuning (Equation (5)), the stochastic differential equation describing the loss dynamics is

$$\partial \mathcal{L}_{\text{ft}} = -(B^T v - X^T Y)^T B^T B (B^T v - X^T Y) \partial t + (B^T v - X^T Y)^T B^T \sqrt{2\sigma^2} \partial W_t \quad (24)$$

$$- (B^T v - X^T Y)^T (B^T v - X^T Y) v^T v \partial t + (B^T v - X^T Y)^T (\sqrt{2\sigma^2} \partial W_t') v \quad (25)$$

$$+ \sigma^2 \|B\|_F^2 \partial t + \sigma^2 d \|v\|_2^2 \partial t. \quad (26)$$

where we use ∂ as the differential sign and use d as the data input dimension.

Proof of Corollary A.3.

$$\partial \mathcal{L}_{\text{ft}} = \partial \frac{1}{2} \|X B^T v - Y\|^2 \quad (27)$$

$$= \frac{1}{2} \langle \nabla_v \|X B^T v - Y\|^2, \partial v \rangle + \frac{1}{2} \langle \nabla_B \|X B^T v - Y\|^2, \text{vec}(\partial B) \rangle \quad (28)$$

$$+ \frac{1}{4} (\partial v)^T H_{\|X B^T v - Y\|^2} (\partial v) + \frac{1}{4} [\text{vec}(\partial B)]^T H_{\|X B^T v - Y\|^2} \text{vec}(\partial B) \quad (29)$$

$$= (X B^T v - Y)^T X B^T \partial v + (X B^T v - Y)^T X (\partial B)^T v \quad (30)$$

$$+ \frac{1}{2} (\partial v)^T B X^T X B^T (\partial v) + \frac{1}{2} [\text{vec}(\partial B)]^T \begin{bmatrix} v_1 \\ 0 \\ \vdots \\ v_k \end{bmatrix} \underbrace{[v_1 \ 0 \ \cdots \ v_k]}_{d \times k} \text{vec}(\partial B) \quad (31)$$

$$= - (B^T v - X^T Y)^T B^T B (B^T v - X^T Y) \partial t + (B^T v - X^T Y)^T B^T \sqrt{2\sigma^2} \partial W_t \quad (32)$$

$$- (B^T v - X^T Y)^T (B^T v - X^T Y) v^T v \partial t + (B^T v - X^T Y)^T (\sqrt{2\sigma^2} \partial W_t') v \quad (33)$$

$$+ \sigma^2 \text{trace}(B B^T) \partial t + \sigma^2 d \|v\|^2 \partial t \quad (34)$$

$$= - (B^T v - X^T Y)^T B^T B (B^T v - X^T Y) \partial t + (B^T v - X^T Y)^T B^T \sqrt{2\sigma^2} \partial W_t \quad (35)$$

$$- (B^T v - X^T Y)^T (B^T v - X^T Y) v^T v \partial t + (B^T v - X^T Y)^T (\sqrt{2\sigma^2} \partial W_t') v \quad (36)$$

$$+ \sigma^2 \|B\|_F^2 \partial t + \sigma^2 d \|v\|_2^2 \partial t \quad (37)$$

□

Remark A.4 (Noise effects on linear networks). In the loss dynamics of fine-tuning (Corollary A.3), the noise induced deterministic terms

$$\sigma^2 (\|B\|_F^2 + d \|v\|_2^2) \partial t$$

does not explicitly depend on the linear head size k . We do a sanity check for this result in a discretized setting (so that we skip Itô's lemma and stochastic calculus). Say we inject noise ΔB to B , where ΔB is a $k \times d$ -matrix, and its entries are independent and follow Gaussian distribution $\mathcal{N}(0, \sigma)$. Then the expectation of the perturbed loss is:

$$\mathbb{E}[\mathcal{L}] = \frac{1}{2} \mathbb{E}[\|X(B + \Delta B)^T v - Y\|^2] \quad (38)$$

$$= \frac{1}{2} \|X B^T v - Y\|^2 + \mathbb{E}[(X B^T v - Y)^T X (\Delta B)^T v] + \frac{1}{2} \mathbb{E}[v^T \Delta B (\Delta B)^T v] \quad (39)$$

$$= \frac{1}{2} \|X B^T v - Y\|^2 + \frac{1}{2} \mathbb{E}[v^T \Delta B (\Delta B)^T v] \quad (40)$$

$$= \frac{1}{2} \|X B^T v - Y\|^2 + \frac{1}{2} \sigma^2 \cdot d \cdot \|v\|^2 \quad (41)$$

A.2 Linear probing loss upper bound

Lemma A.5 ((Strong) convexity of linear probing phase)

The empirical risk $\mathcal{L} = \frac{1}{2} \sum_{i=1}^n \ell(f(x_i), y_i)$ is 1-strongly convex.

Lemma A.6 (Initial loss before linear probing)

If Assumption 3.3 holds, then the expected empirical risk before linear probing is

$$\mathbb{E}[\mathcal{L}_0] = \frac{1}{2} (k\beta + \|Y\|^2) \quad (42)$$

Proof of Lemma A.6. We initialize the linear head with a Gaussian distribution $\mathcal{N}(0, \beta I_{k \times k})$. So the expected initial loss is:

$$\mathbb{E}[\mathcal{L}_0] = \frac{1}{2} \mathbb{E}[\|X B_0^T v_0 - Y\|^2] \quad (43)$$

$$= \frac{1}{2} \mathbb{E}[v_0^T B_0 X^T X B_0^T v_0 + Y^T Y - 2Y^T X B_0^T v_0] \quad (44)$$

$$= \frac{1}{2} \mathbb{E}[v_0^T B_0 B_0^T v_0 + Y^T Y] \quad (45)$$

$$= \frac{1}{2} \mathbb{E}[v_0^T v_0 + Y^T Y] = \frac{1}{2} (k\beta + \|Y\|^2) \quad (46)$$

□

Theorem A.7 (Expected loss upper bound of linear probing)

The expected empirical risk in linear probing is upper bounded by

$$\mathbb{E}[\mathcal{L}_{\text{lp}}(t)] \leq e^{-t} \mathbb{E}[\mathcal{L}_0] + (1 - e^{-t})(\gamma + k\sigma^2) \quad (47)$$

Proof of Theorem 3.10. By Lemma A.5, \mathcal{L} is 1-strongly convex, we have the Lojasiewicz inequality

$$\mathcal{L}(v) - \{\min_v \mathcal{L}\} \leq \frac{1}{2} \|\nabla_v \mathcal{L}(v)\|_2^2 \quad (48)$$

For simplicity, we denote $\mathbb{E}[\mathcal{L}] := \hat{\mathcal{L}}$. Consider the Langevin diffusion in Equation (4) when $\mathcal{L}(v) - \{\min_v \mathcal{L}\} - k\sigma^2 > 0$, by Corollary A.2:

$$\partial \mathcal{L}(v) = \langle \nabla_v \mathcal{L}(v), -\nabla_v \mathcal{L}(v) \partial t + \sqrt{2\sigma^2} \partial W_t \rangle + k\sigma^2 \partial t \quad (49)$$

$$\partial \mathcal{L}(v) \leq -\|\nabla_v \mathcal{L}(v)\|_2^2 \partial t + \langle \nabla_v \mathcal{L}(v), \sqrt{2\sigma^2} \partial W_t \rangle + k\sigma^2 \partial t \quad (50)$$

$$\text{//By Lojasiewicz inequality} \quad (51)$$

$$\partial \mathcal{L}(v) \leq (-\mathcal{L}(v) + \{\min_v \mathcal{L}\}) \partial t + \langle \nabla_v \mathcal{L}(v), \sqrt{2\sigma^2} \partial W_t \rangle + k\sigma^2 \partial t \quad (52)$$

$$\partial(\mathbb{E}[\mathcal{L}(v)] - \{\min_v \mathcal{L}\} - k\sigma^2) \leq -(\mathbb{E}[\mathcal{L}(v)] - \{\min_v \mathcal{L}\}) \partial t + k\sigma^2 \partial t \quad (53)$$

$$\partial(\hat{\mathcal{L}} - \{\min_v \mathcal{L}\} - k\sigma^2) \leq -(\hat{\mathcal{L}} - \{\min_v \mathcal{L}\} - k\sigma^2) \partial t \quad (54)$$

$$\text{//When } \hat{\mathcal{L}} - \{\min_v \mathcal{L}\} - k\sigma^2 > 0 \quad (55)$$

$$\partial \ln |\hat{\mathcal{L}} - \{\min_v \mathcal{L}\} - k\sigma^2| \leq -1 \partial t \quad (56)$$

$$\ln |\hat{\mathcal{L}} - \{\min_v \mathcal{L}\} - k\sigma^2| \leq \ln |\widehat{\mathcal{L}}(v_0) - \{\min_v \mathcal{L}\} - k\sigma^2| - t \quad (57)$$

$$\hat{\mathcal{L}} - \{\min_v \mathcal{L}\} - k\sigma^2 \leq e^{-t} (\widehat{\mathcal{L}}(v_0) - \{\min_v \mathcal{L}\} - k\sigma^2) \quad (58)$$

$$\hat{\mathcal{L}} \leq e^{-t} (\widehat{\mathcal{L}}(v_0) - \{\min_v \mathcal{L}\} - k\sigma^2) + \{\min_v \mathcal{L}\} + k\sigma^2 \quad (59)$$

$$\hat{\mathcal{L}} \leq e^{-t} \widehat{\mathcal{L}}(v_0) + (1 - e^{-t})(\{\min_v \mathcal{L}\} + k\sigma^2) \quad (60)$$

$$\hat{\mathcal{L}} \leq e^{-t} \widehat{\mathcal{L}}(v_0) + (1 - e^{-t})(\gamma + k\sigma^2) \quad (61)$$

□

Corollary A.8 (Expected loss upper bound of linear probing from Kaiming initialization)

If Assumption 3.3 holds, then the expected loss is upper bounded by

$$\mathbb{E}[\mathcal{L}_{\text{lp}}(t)] \leq \frac{1}{2}(k\beta + \|Y\|^2)e^{-t} + (1 - e^{-t})(\gamma + k\sigma^2) \quad (62)$$

Proof of Corollary A.8. The result is immediate when we combine Lemma A.6 and Theorem 3.10. □

A.3 Imbalance matrix from linear probing

Lemma A.9 (Eigenvalues of imbalance matrix at the beginning of fine-tuning)

During the linear probing phase (Equation (4)), for the imbalance matrix defined in Definition 3.5,

1. the minimum eigenvalue of the imbalance matrix is always -1 ;
2. other eigenvalues evolve in this way:

$$\mathbb{E}[\lambda] = \mathbb{E}[\|v\|_2^2] - 1 \geq -1 \quad (63)$$

Proof of Lemma A.9. Consider any eigenpair (λ, u) of matrix D , we have

$$Du = \lambda u \quad (64)$$

$$(vv^T - B_0 B_0^T)u = \lambda u \quad (65)$$

$$(vv^T - I_{k \times k})u = \lambda u \quad (66)$$

$$(v^T u)v = (\lambda + 1)u \quad (67)$$

$$(68)$$

We can take any $u \perp v$ and $(u, -1)$ is an eigenpair of D . So -1 is always an eigenvalue of D . We need to discuss two different cases here:

1. If $\lambda = -1$, we only know that $u \perp v$.

2. If $\lambda \neq -1$, then v and u are parallel. Say $u = \alpha v$, then

$$u = \frac{v^T u}{\lambda + 1} v \quad (69)$$

$$\alpha v = \frac{\alpha \|v\|_2^2}{\lambda + 1} v \quad (70)$$

$$\implies \lambda = \|v\|_2^2 - 1 \geq -1 \quad (71)$$

□

Proposition A.10 (Expected eigenvalue of imbalance matrix at the beginning of fine-tuning)
Say we run linear probing for time t . If Assumption 3.3 holds, then for the imbalance matrix defined in Definition 3.5, we have

$$\mathbb{E}[\|v\|^2] = k\beta e^{-2t} + 2\|B_0 X^T Y\|^2 (e^{-t} - e^{-2t}) + (\|B_0 X^T Y\|^2 + k\sigma^2)(1 - e^{-2t}) \quad (72)$$

throughout the linear probing process. Then by Lemma A.9, for those eigenvalues not equal to -1 , we have

$$\mathbb{E}[\lambda] = \mathbb{E}[\|v\|_2^2] - 1 = k\beta e^{-2t} + 2\|B_0 X^T Y\|^2 (e^{-t} - e^{-2t}) + (\|B_0 X^T Y\|^2 + k\sigma^2)(1 - e^{-2t}) - 1 \quad (73)$$

at the beginning of fine-tuning after linear probing.

Proof of Proposition A.10. By Equation (4), the Langevin diffusion of linear probing is:

$$\partial v = -B_0 X^T (X B_0^T v - Y) \partial t + \sqrt{2\sigma^2} \partial W_t = -v \partial t + B_0 X^T Y \partial t + \sqrt{2\sigma^2} \partial W_t \quad (74)$$

We consider the evolution of $v^T v$: by Itô's formula (Equation (A.1))

$$\partial v^T v = 2v^T \partial v + (\partial v)^T I_k (\partial v) \quad (75)$$

$$\partial v^T v = -2v^T (v - B_0 X^T Y) \partial t + 2v^T \sqrt{2\sigma^2} \partial W_t + 2k\sigma^2 \partial t \quad (76)$$

$$\partial v^T v = (-2v^T v + 2v^T B_0 X^T Y) \partial t + 2v^T \sqrt{2\sigma^2} \partial W_t + 2k\sigma^2 \partial t \quad (77)$$

To solve the above equation, we need to solve the dynamics of $v^T B_0 X^T Y$:

$$\partial Y^T X B_0^T v = -Y^T X B_0^T (v - B_0 X^T Y) \partial t + \sqrt{2\sigma^2} \partial W_t \quad (78)$$

$$\partial \mathbb{E}[Y^T X B_0^T v] = -\mathbb{E}[Y^T X B_0^T v] \partial t + \|B_0 X^T Y\|^2 \partial t \quad (79)$$

$$\frac{\partial}{\partial t} \mathbb{E}[Y^T X B_0^T v - \|B_0 X^T Y\|^2] = -\mathbb{E}[Y^T X B_0^T v - \|B_0 X^T Y\|^2] \quad (80)$$

$$\frac{\partial}{\partial t} \ln |\mathbb{E}[Y^T X B_0^T v - \|B_0 X^T Y\|^2]| = -1 \quad (81)$$

$$|\mathbb{E}[Y^T X B_0^T v_t - \|B_0 X^T Y\|^2]| = |\mathbb{E}[Y^T X B_0^T v_0 - \|B_0 X^T Y\|^2]| \cdot \exp(-t) \quad (82)$$

When Assumption 3.3 holds, $\mathbb{E}[Y^T X B_0^T v_0] = 0$. Then

$$|\mathbb{E}[Y^T X B_0^T v_t - \|B_0 X^T Y\|^2]| = |\mathbb{E}[Y^T X B_0^T v_0 - \|B_0 X^T Y\|^2]| \cdot \exp(-t) \quad (83)$$

$$\mathbb{E}[\|B_0 X^T Y\|^2 - Y^T X B_0^T v_t] = \mathbb{E}[\|B_0 X^T Y\|^2 - Y^T X B_0^T v_0] \cdot \exp(-t) \quad (84)$$

So we can rewrite Equation (77) as:

$$\partial \mathbb{E}[\|v\|^2] = (-2\mathbb{E}[\|v\|^2] + 2\mathbb{E}[v^T B_0 X^T Y]) \partial t + 2k\sigma^2 \partial t \quad (85)$$

$$\partial \mathbb{E}[\|v\|^2] = (-2\mathbb{E}[\|v\|^2] + 2(\mathbb{E}[\|B_0 X^T Y\|^2 - Y^T X B_0^T v_0] \cdot \exp(-t) + \|B_0 X^T Y\|^2)) \partial t + 2k\sigma^2 \partial t \quad (86)$$

$$\frac{1}{2} \frac{\partial}{\partial t} \mathbb{E}[\|v\|^2] = -\mathbb{E}[\|v\|^2] + \mathbb{E}[\|B_0 X^T Y\|^2 - Y^T X B_0^T v_0] \cdot \exp(-t) + (\|B_0 X^T Y\|^2 + k\sigma^2) \quad (87)$$

Let $a_1 = \mathbb{E}[\|B_0 X^T Y\|^2 - Y^T X B_0^T v_0]$, $a_2 = \|B_0 X^T Y\|^2 + k\sigma^2$, $f(t) = \mathbb{E}[\|v\|^2]$ and rewrite the above equation:

$$\frac{1}{2} f'(t) + f(t) = a_1 e^{-t} + a_2 \quad (88)$$

$$f'(t) + 2f(t) = 2a_1e^{-t} + 2a_2 \quad (89)$$

$$e^{2t}f'(t) + 2e^{2t}f(t) = 2a_1e^t + 2a_2e^{2t} \quad (90)$$

$$e^{2t}f(t) \Big|_0^t = (2a_1e^t + a_2e^{2t}) \Big|_0^t \quad (91)$$

$$e^{2t}f(t) = f(0) + 2a_1(e^t - 1) + a_2(e^{2t} - 1) \quad (92)$$

$$f(t) = f(0)e^{-2t} + 2a_1(e^{-t} - e^{-2t}) + a_2(1 - e^{-2t}) \quad (93)$$

by Assumption 3.3 we have $f(0) = k\beta$ and $a_1 = \|B_0X^TY\|^2$. \square

Lemma A.11 (Imbalance matrix in fine-tuning)

During fine-tuning (Equation (5)), the imbalance matrix D in Definition 3.5 evolves as

$$\frac{\partial}{\partial t}\mathbb{E}[D] = (1-d)\sigma^2I_{k \times k} \quad (94)$$

where d is the dimension of data inputs ($B \in \mathbb{R}^{k \times d}$).

Proof of Lemma 3.6. We prove this lemma by analyzing the infinitesimal generator A of imbalance matrix D at any time:

$$A(D)_{ij} := \lim_{t \downarrow 0} \frac{\mathbb{E}^D[(D(t))_{ij}] - (D)_{ij}}{t} \quad (95)$$

$$= 0 + \sigma^2 \sum_{i' \in [k]} \sum_{j' \in [k]} \mathbf{1}[i' = j' = i = j] \quad (96)$$

$$- \sigma^2 \sum_{i' \in [k], j' \in [d]} \sum_{i'' \in [k], j'' \in [d]} \mathbf{1}[i' = i'' = i = j \text{ and } j' = j''] \quad (97)$$

the generator is zero for $i \neq j$. So we can just consider the case where $i = j$.

$$A(D)_{ii} = \sigma^2 \sum_{i' \in [k]} \sum_{j' \in [k]} \mathbf{1}[i' = j' = i] \quad (98)$$

$$- \sigma^2 \sum_{i' \in [k], j' \in [d]} \sum_{i'' \in [k], j'' \in [d]} \mathbf{1}[i' = i'' = i \text{ and } j' = j''] \quad (99)$$

$$= (1-d)\sigma^2 \quad (100)$$

\square

Lemma A.12 (Monotonic eigenvalue of imbalance matrix in fine-tuning)

Denote D_{lp} as the imbalance matrix right after linear probing phase. All eigenvalues of the imbalance matrix are decreasing in expectation during fine-tuning. Specifically,

$$\mathbb{E}[\lambda(D)] = \mathbb{E}[\lambda(D_{\text{lp}})] + (1-d)\sigma^2t \quad (101)$$

where t is the time-span of fine-tuning process.

Proof of Lemma A.12. Pick any eigenpair (λ, u) of imbalance matrix D (Definition 3.5) such that $\|u\|_2 = 1$. By Itô's lemma (Equation (A.1)):

$$\partial \lambda = u^T(\partial D)u + u^T(\partial D)(\lambda I - D)^\dagger(\partial D)u^T \quad (102)$$

$$= (1-d)\sigma^2\|u\|_2^2\partial t + \partial M_t + (1-d)^2\sigma^4u^T(\lambda I - D)^\dagger u^T \quad (103)$$

$$= (1-d)\sigma^2\partial t + \partial M_t + (1-d)^2\sigma^4u^T(\lambda I - D)^\dagger u^T \quad (104)$$

where M_t is the martingale induced by the Brownian noise and $(\cdot)^\dagger$ denotes the pseudo inverse of a certain matrix. Say the the singular value decomposition (SVD) of D is

$$D = U\Sigma U^T = U \begin{bmatrix} \lambda_1 & & \mathbf{0} \\ & \lambda_2 & \\ \mathbf{0} & & \ddots \end{bmatrix} U^T \quad (105)$$

where we have $\lambda \in \text{diag}\Sigma$ and u being a column vector in U . So we can write the SVD of $(\lambda I - D)$ as:

$$\lambda I - D = V\Sigma'V^T = V \begin{bmatrix} \lambda - \lambda_1 & & \mathbf{0} \\ & \lambda - \lambda_2 & \\ \mathbf{0} & & \ddots \end{bmatrix} V^T \quad (106)$$

where we obtain V by removing u in the columns of U and we obtain Σ' by removing λ in Σ . Then the pseudo inverse of $(\lambda I - D)$ is

$$(\lambda I - D)^\dagger = V\Sigma'V^T = V \begin{bmatrix} \frac{1}{\lambda - \lambda_1} & & \mathbf{0} \\ & \frac{1}{\lambda - \lambda_2} & \\ \mathbf{0} & & \ddots \end{bmatrix} V^T \quad (107)$$

Since U is orthogonal, we shall have $V^T u = \mathbf{0}$. Then we can rewrite the stochastic dynamics of D as:

$$\frac{\partial}{\partial t} \mathbb{E}[\lambda] = (1 - d)\sigma^2 \quad (108)$$

□

A.4 Fine-tuning loss

Lemma A.13 (Bounding the norm of linear head $\|v\|_2^2$)

During fine-tuning (Equation (5)), we can bound the norm of $\|v\|_2^2$ with the imbalance matrix D in Definition 3.5 as

$$\frac{\underline{\lambda} + \sqrt{\underline{\lambda}^2 + 4\|w\|^2}}{2} \leq \|v\|_2^2 \leq \frac{\bar{\lambda} + \sqrt{\bar{\lambda}^2 + 4\|w\|^2}}{2} \quad (109)$$

where we denote $\underline{\lambda} = \lambda_{\min}(\hat{D})$, $\bar{\lambda} = \lambda_{\max}(\hat{D})$.

Proof of Lemma A.13. Given the information of imbalance matrix, we can bound the linear head norm. Denote $\underline{\lambda} = \lambda_{\min}(D)$, $\bar{\lambda} = \lambda_{\max}(D)$. Denote $w = B^T v$ and multiply D with v on both sides:

$$v^T D v = (v^T v)^2 - (v^T B)(B^T v) \quad (110)$$

$$v^T D v = \|v\|_2^4 - \|w\|_2^2 \quad (111)$$

We have a range for the Rayleigh quotient: $\frac{x^T D x}{x^T x} \in [\underline{\lambda}, \bar{\lambda}]$. So we obtain two inequalities:

$$\begin{cases} \|v\|_2^4 - \|w\|_2^2 \geq \underline{\lambda} \|v\|_2^2 \\ \|v\|_2^4 - \|w\|_2^2 \leq \bar{\lambda} \|v\|_2^2 \end{cases} \quad (112)$$

$$= \begin{cases} \|v\|_2^4 - \underline{\lambda} \|v\|_2^2 - \|w\|_2^2 \geq 0 \\ \|v\|_2^4 - \bar{\lambda} \|v\|_2^2 - \|w\|_2^2 \leq 0 \end{cases} \quad (113)$$

To get a lower bound of v , we can solve two quadratic inequalities. For the first quadratic equation, since the smaller root is non-positive, $\underline{\lambda} - \sqrt{\underline{\lambda}^2 + 4\|w\|^2} \leq 0$, we just bound $\|v\|_2^2$ with the larger root:

$$\|v\|_2^2 \geq \frac{\underline{\lambda} + \sqrt{\underline{\lambda}^2 + 4\|w\|^2}}{2} \quad (114)$$

similarly, for the second quadratic equation, we obtain an upper bound for $\|v\|_2^2$ with the right-side zero point:

$$\|v\|_2^2 \leq \frac{\bar{\lambda} + \sqrt{\bar{\lambda}^2 + 4\|w\|^2}}{2} \quad (115)$$

□

Lemma A.14 (Bounding eigenvalues of $B^T B$ (re-stated from [64]))

During fine-tuning (Equation (5)), we can bound any nonzero eigenvalue λ_i of $B^T B$ as

$$\lambda_i \in \left[\frac{-\bar{\lambda} + \sqrt{\bar{\lambda}^2 + 4(z_i^T w)^2}}{2}, \frac{-\underline{\lambda} + \sqrt{\underline{\lambda}^2 + 4(z_i^T w)^2}}{2} \right] \quad (116)$$

where we use the imbalance matrix D in Definition 3.5 and denote

$$\begin{cases} \bar{\lambda} = \lambda_{\max}(D) \\ \underline{\lambda} = \lambda_{\min}(D) \end{cases} \quad (117)$$

Proof of Lemma A.14. The proof of this lemma follows the proof of Lemma 3 in [64]. $B^T B$ is symmetric and positive semidefinite ($x^T B^T B x = \|Bx\|_2^2 \geq 0$). So every eigenvalue of $B^T B$ is non-negative.

D has at most one positive eigenvalue: if D has more than one eigenvalues, then the subspace of \mathbb{R}^k spanned by the all positive eigenvectors has dimension at least 2, which must have non-trivial intersection with $\ker(v^T)$ as $\dim(\ker(v^T)) = k - 1$. Then there exists a nonzero vector $z \in \ker(v^T)$ such that $z^T D z > 0$, which would imply $-z^T B B^T z = z^T D z > 0$, a contradiction.

For any eigenvalue-eigenvector pair (λ_i, z_i) of $B^T B$ where $\lambda_i \neq 0$ and $z_i \in \mathbb{S}^{d-1}$,

$$\lambda_i^2 = z_i^T (B^T B)^2 z_i \quad (118)$$

$$\text{//replace something with imbalance matrix} \quad (119)$$

$$\lambda_i^2 = (z_i^T w)^2 - z_i^T B^T D B z_i \quad (120)$$

$$\lambda_i^2 - (z_i^T w)^2 = -z_i^T B^T D B z_i \quad (121)$$

$$\lambda_i^2 - (z_i^T w)^2 \in (z_i^T (B^T B) z_i) \cdot [-\lambda_{\max}, -\lambda_{\min}] \quad (122)$$

$$\lambda_i^2 - (z_i^T w)^2 \in \lambda_i \cdot [-\lambda_{\max}, -\lambda_{\min}] \quad (123)$$

again, we can rewrite this as two quadratic inequalities

$$\begin{cases} \lambda_i^2 + \lambda_{\max} \lambda_i - (z_i^T w)^2 \geq 0 \\ \lambda_i^2 + \lambda_{\min} \lambda_i - (z_i^T w)^2 \leq 0 \end{cases} \quad (124)$$

from them we know that there are two possible intervals:

$$\begin{cases} \lambda_i \in \left[-\infty, \frac{-\lambda_{\max} - \sqrt{\lambda_{\max}^2 + 4(z_i^T w)^2}}{2} \right] \cup \left[\frac{-\lambda_{\max} + \sqrt{\lambda_{\max}^2 + 4(z_i^T w)^2}}{2}, +\infty \right] \\ \lambda_i \in \left[\frac{-\lambda_{\min} - \sqrt{\lambda_{\min}^2 + 4(z_i^T w)^2}}{2}, \frac{-\lambda_{\min} + \sqrt{\lambda_{\min}^2 + 4(z_i^T w)^2}}{2} \right] \end{cases} \quad (125)$$

Note that we must have $\lambda_i \geq 0$ since $B^T B$ is positive semidefinite. So we can rewrite the bounds:

$$\lambda_i \in \left[\frac{-\lambda_{\max} + \sqrt{\lambda_{\max}^2 + 4(z_i^T w)^2}}{2}, \frac{-\lambda_{\min} + \sqrt{\lambda_{\min}^2 + 4(z_i^T w)^2}}{2} \right] \quad (126)$$

since the function $f(x) = -x + \sqrt{x^2 + c^2}$ is monotonically decreasing, we have $f(\lambda_{\max}) \leq f(\lambda_{\min})$, i.e. the lower bound is no greater than the upper bound, i.e. the above interval is always non-empty. \square

A.5 Layerwise sensitivity

Lemma A.15 (Sensitivity upper bounds for two-layer linear networks)

Consider two neighboring and normalized datasets $\mathcal{D} = (X, Y)$ and $\mathcal{D}' = (X', Y')$ where $X, X' \in \{A^T A = I_{d \times d} : A \in \mathbb{R}^{n \times d}\}$ and $\|Y\|_2 = \|Y'\|_2 = 1$. Then the L_2 -distance of each layer is upper bounded by

$$\begin{cases} \|\nabla_B \mathcal{L}(v, B; \mathcal{D}) - \nabla_B \mathcal{L}(v, B; \mathcal{D}')\|_2 \leq \|v\|_2 \|(X')^T Y' - X^T Y\|_2 \\ \|\nabla_v \mathcal{L}(v, B; \mathcal{D}) - \nabla_v \mathcal{L}(v, B; \mathcal{D}')\|_2 \leq \|B\|_2 \|(X')^T Y' - X^T Y\|_2 \end{cases} \quad (127)$$

Proof of Lemma A.15. The L_2 -distance of B -layer gradients are

$$\begin{aligned}
& \|\nabla_B \mathcal{L}(v, B; X) - \nabla_B \mathcal{L}(v, B; X')\|_2 \\
&= \|v(XB^T v - Y)^T X - v(X'B^T v - Y')^T X'\|_2 \\
&= \|v(X^T X B^T v - X^T Y)^T - v((X')^T X' B^T v - (X')^T Y')^T\|_2 \\
&\leq \|v\|_2 \|X^T X B^T v - X^T Y - (X')^T X' B^T v + (X')^T Y'\|_2 \\
&= \|v\|_2 \|(X')^T Y' - X^T Y\|_2
\end{aligned}$$

Similarly, the L_2 -distance of v -layer gradients are

$$\|\nabla_v \mathcal{L}(v, B; X) - \nabla_v \mathcal{L}(v, B; X')\|_F \leq \|B\|_F \|X^T X B^T v - X^T Y - (X')^T X' B^T v + (X')^T Y'\|_2 \quad (128)$$

$$= \|B\|_F \|(X')^T Y' - X^T Y\|_2 \quad (129)$$

□

Proof of Proposition 3.7. At the initialization of full fine-tuning, we have $\|B_0\|_F = k$ and $\|v_0\|_2 = k/\sqrt{d}$. When we pick $\mathcal{D}, \mathcal{D}'$ such that $X = X', Y \parallel v_0$ and $Y' = -Y$, we have

$$\|\nabla_B \mathcal{L}(v_0, B_0; \mathcal{D}) - \nabla_B \mathcal{L}(v_0, B_0; \mathcal{D}')\|_2 = \sqrt{2}\|v_0\|_2 \quad (130)$$

So we can bound the local sensitivity of $\nabla_B \mathcal{L}$ at (v_0, B_0) by:

$$\Delta(\nabla_B \mathcal{L}(v_0, B_0)) := \sup_{\mathcal{D}, \mathcal{D}'} \|\nabla_B \mathcal{L}(v_0, B_0; \mathcal{D}) - \nabla_B \mathcal{L}(v_0, B_0; \mathcal{D}')\|_2 \in \left[\sqrt{2}\|v_0\|_2, 2\|v_0\|_2 \right] \quad (131)$$

By taking expectation on v_0 , we get $\mathbb{E}[\Delta(\nabla_B \mathcal{L}(v_0, B_0))] \in \left[k\sqrt{2/d}, 2k/\sqrt{d} \right]$. When we pick $\mathcal{D}, \mathcal{D}'$ such that $X = X', (1, Y)$ being an eigenvalue-eigenvector pair of B_0 , and $Y = -Y'$, we have

$$\|\nabla_v \mathcal{L}(v_0, B_0; \mathcal{D}) - \nabla_v \mathcal{L}(v_0, B_0; \mathcal{D}')\|_2 = \sqrt{2}k \quad (132)$$

So we can bound the local sensitivity of $\nabla_v \mathcal{L}$ at (v_0, B_0) by:

$$\Delta(\nabla_v \mathcal{L}(v_0, B_0)) := \sup_{\mathcal{D}, \mathcal{D}'} \|\nabla_v \mathcal{L}(v_0, B_0; \mathcal{D}) - \nabla_v \mathcal{L}(v_0, B_0; \mathcal{D}')\|_2 \in \left[\sqrt{2}k, 2k \right] \quad (133)$$

Combining the bounds of local sensitivities of $\nabla_v \mathcal{L}$ and $\nabla_B \mathcal{L}$, we have

$$\Delta(\nabla_v \mathcal{L}(v_0, B_0)) = \Theta(\sqrt{d}\Delta(\nabla_B \mathcal{L}(v_0, B_0))) \quad (134)$$

□

A.6 Fine-tuning loss upper bound

Lemma A.16 (Imbalance matrix in fine-tuning under layerwise noise)

During fine-tuning (Equation (10)), the imbalance matrix D in Definition 3.5 evolves as

$$\mathbb{E} \left[\frac{dD}{dt} \right] = 0 \quad (135)$$

Proof of Lemma 3.9. We prove this lemma by analyzing the infinitesimal generator A of imbalance matrix D :

$$A(D_0(v, B))_{ij} := \lim_{t \downarrow 0} \frac{\mathbb{E}^{D_0}[D_{ij}] - (D_0)_{ij}}{t} \quad (136)$$

$$= 0 + \sigma^2 \sum_{i' \in [k]} \sum_{j' \in [k]} \mathbf{1}[i' = j' = i = j] \quad (137)$$

$$- \sigma^2 \sum_{i' \in [k], j' \in [d]} \sum_{i'' \in [k], j'' \in [d]} \mathbf{1}[i' = i'' = i = j \text{ and } j' = j''] \quad (138)$$

the generator is zero for $i \neq j$. So we can just consider the case where $i = j$.

$$A(D_0(v, B))_{ii} = \sigma^2 \sum_{i' \in [k]} \sum_{j' \in [k]} \mathbf{1}[i' = j' = i] \quad (139)$$

$$- \sigma^2 \sum_{i' \in [k], j' \in [d]} \sum_{i'' \in [k], j'' \in [d]} \mathbf{1}[i' = i'' = i \text{ and } j' = j''] \quad (140)$$

$$= (d - d)\sigma^2 \quad (141)$$

$$= 0 \quad (142)$$

□

Theorem A.17 (Loss upper bound of fine-tuning)

In fine-tuning under layerwise noise (Equation (10)), we have

$$\mathbb{E}[\mathcal{L}] \lesssim \mathbb{E}[\mathcal{L}]e^{(-\bar{\lambda} + \sqrt{2}\sigma^2(1+d))t} + L^\square(1 - e^{(-\bar{\lambda} + \sqrt{2}\sigma^2(1+d))t}) \quad (143)$$

where $L^\square = \sigma^2 \frac{(1+d)\|X^T Y\| - d\bar{\lambda}}{\bar{\lambda} - \sqrt{2}\sigma^2(1+d)}$.

Proof of Theorem 3.11. We first simplify the loss dynamics:

$$\partial \mathcal{L} = \partial \frac{1}{2} \|XB^T v - Y\|^2 \quad (144)$$

$$= \frac{1}{2} \langle \nabla_v \|XB^T v - Y\|^2, \partial v \rangle + \frac{1}{2} \langle \nabla_B \|XB^T v - Y\|^2, \text{vec}(\partial B) \rangle \quad (145)$$

$$+ \frac{1}{4} (\partial v)^T H_{\|XB^T v - Y\|^2} (\partial v) + \frac{1}{4} [\text{vec}(\partial B)]^T H_{\|XB^T v - Y\|^2} \text{vec}(\partial B) \quad (146)$$

$$= (XB^T v - Y)^T XB^T \partial v + (XB^T v - Y)^T X (\partial B)^T v \quad (147)$$

$$+ \frac{1}{2} (\partial v)^T BB^T (\partial v) + \frac{1}{2} [\text{vec}(\partial B)]^T H_{\|XB^T v - Y\|^2} \text{vec}(\partial B) \quad (148)$$

$$= - (XB^T v - Y)^T XB^T BX^T (XB^T v - Y) \partial t + (XB^T v - Y)^T XB^T \sqrt{2\sigma^2 d} \partial W_t \quad (149)$$

$$- (XB^T v - Y)^T X X^T (XB^T v - Y) v^T v \partial t + (XB^T v - Y)^T X (\sqrt{2\sigma^2} \partial W_t') v \quad (150)$$

$$+ \sigma^2 \text{trace}(BB^T) \partial t + \sigma^2 d \|v\|^2 \partial t \quad (151)$$

$$= - (B^T v - X^T Y)^T B^T B (B^T v - X^T Y) \partial t + (B^T v - X^T Y)^T B^T \sqrt{2\sigma^2} \partial W_t \quad (152)$$

$$- (B^T v - X^T Y)^T (B^T v - X^T Y) v^T v \partial t + (B^T v - X^T Y)^T (\sqrt{2\sigma^2} \partial W_t') v \quad (153)$$

$$+ \sigma^2 \text{trace}(B^T B) \partial t + \sigma^2 d \|v\|^2 \partial t \quad (154)$$

By Lemma A.13 and Lemma A.14, we have

$$\partial \mathbb{E} \mathcal{L} = - \mathbb{E}[(w - X^T Y)^T (B^T B + v^T v I_{d \times d})(w - X^T Y)] \partial t + \sigma^2 \mathbb{E}[\|B\|_F^2 + d\|v\|_2^2] \partial t \quad (155)$$

$$\leq \mathbb{E} \left\{ - \|w - X^T Y\|_2^2 \frac{\bar{\lambda} + \sqrt{\bar{\lambda}^2 + 4\|w\|^2}}{2} \partial t - \|w - X^T Y\|_2^2 \frac{-\bar{\lambda} + \sqrt{\bar{\lambda}^2 + 4(z_{\min}^T w)^2}}{2} \partial t \right\} \quad (156)$$

$$+ \mathbb{E} \left\{ \sigma^2 d \frac{-\bar{\lambda} + \sqrt{\bar{\lambda}^2 + 4(z_{\min}^T w)^2}}{2} \partial t + \sigma^2 d \frac{\bar{\lambda} + \sqrt{\bar{\lambda}^2 + 4\|w\|^2}}{2} \partial t \right\} \quad (157)$$

$$\leq - \frac{1}{2} \mathbb{E}[\|w - X^T Y\|_2^2 (\Lambda_{\min} + \Lambda_{\max})] \partial t + \frac{1}{2} \sigma^2 \mathbb{E}[d\Gamma_{\min} + \Gamma_{\max}] \partial t \quad (158)$$

where we define

$$\begin{cases} \Lambda_{\min} = \bar{\lambda} + \sqrt{\bar{\lambda}^2 + 4\|w\|^2} \geq \max(0, 2\bar{\lambda}) \\ \Lambda_{\max} = -\bar{\lambda} + \sqrt{\bar{\lambda}^2 + 4(z_{\min}^T w)^2} \geq \max(0, -2\bar{\lambda}) \\ \Gamma_{\min} = -\bar{\lambda} + \sqrt{\bar{\lambda}^2 + 4(z_{\min}^T w)^2} \leq \max(2\|w\|, 2\|w\| - 2\bar{\lambda}) = 2\|w\| + 2\max(0, -\bar{\lambda}) \\ \Gamma_{\max} = \bar{\lambda} + \sqrt{\bar{\lambda}^2 + 4\|w\|^2} \leq \max(2\|w\|, 2\|w\| + 2\bar{\lambda}) = 2\|w\| + 2\max(0, \bar{\lambda}) \end{cases} \quad (159)$$

Then we rewrite the upper bound:

$$\partial\mathbb{E}[\mathcal{L}] \leq -\frac{1}{2}\mathbb{E}[\|w - X^T Y\|_2^2(\Lambda_{\min} + \Lambda_{\max})]\partial t + \frac{1}{2}\sigma^2\mathbb{E}[d\Gamma_{\min} + \Gamma_{\max}]\partial t \quad (160)$$

$$\partial\mathbb{E}[\mathcal{L}] \lesssim -\bar{\lambda}\mathbb{E}[\mathcal{L}]\partial t + \sigma^2(\sqrt{2}(1+d)\mathbb{E}[\mathcal{L}]^{1/2} + (1+d)\|X^T Y\| - d\bar{\lambda})\partial t \quad (161)$$

$$\partial\mathbb{E}[\mathcal{L}] \lesssim (-\bar{\lambda} + \sqrt{2}\sigma^2(1+d))\mathbb{E}[\mathcal{L}]\partial t + \sigma^2((1+d)\|X^T Y\| - d\bar{\lambda})\partial t \quad (162)$$

$$\mathbb{E}[\mathcal{L}] \lesssim \mathbb{E}[\mathcal{L}]e^{(-\bar{\lambda} + \sqrt{2}\sigma^2(1+d))t} + L^\square(1 - e^{(-\bar{\lambda} + \sqrt{2}\sigma^2(1+d))t}) \quad (163)$$

where $L^\square = \sigma^2 \frac{(1+d)\|X^T Y\| - d\bar{\lambda}}{\bar{\lambda} - \sqrt{2}\sigma^2(1+d)}$. □

B More information on experiments

This Appendix provides additional information regarding the datasets, pretraining methods, and adaptation methods.

B.1 Dataset and method details

- ImageNet-1K→CIFAR-10/STL-10. We pretrain the feature extractor without privacy mechanisms on ImageNet-1K and privately fine-tune the feature extractor and a linear head on CIFAR-10.
 - ResNet-50: We consider unsupervised pretraining methods and use a larger model architecture for this benchmark. We initialize pretrained features of ResNet-50 from MoCo-v2 [21] & MoCo-v3 [22] on ImageNet-1K [73] without privacy mechanisms and then privately fine-tune the ResNet-50 model on CIFAR-10 for 10 epochs.
 - Mini-DeiT-Ti: We run Vision Transformer (ViT) models like mini Data-efficient image Transformers (Mini-DeiT) on ImageNet-1K→STL-10 benchmark [78, 94]. We first pretrain a DeiT model on ImageNet then pretrain a Mini-DeiT-Ti model with weight distillation from the DeiT model [94]. The weight of the Mini-DeiT-Ti model is publicly available in the official Github repository of Zhang et al. [94]. After that, we privately fine-tune the Mini-DeiT-Ti model on STL-10 for 20 epochs.
- CIFAR-10→STL-10. This benchmark has been extensively studied in the context of domain adaptation [35, 52]. We pretrain the feature extractor on CIFAR-10 [51] using stochastic gradient descent without privacy mechanisms. Then we finetune the pretrained features and a randomly initialized linear head on STL-10 for 10 epochs [26]. The training subset of STL-10 is small and only contains 500 images. To align with the small scale fine-tuning data, we run the experiments with smaller and data-efficient models: MobileNet-v3 and ResNet-18.
- RandP→CIFAR-10. To verify the general existence of concave utility curves, we also consider a slightly non-standard pretraining protocol: pretrain a wide residual network (WRN) [92] on synthetic images generated by random diffusion processes. We basically follow the experiment settings in [76] and reproduce their results. We first sample synthetic images from StyleGAN-based datasets and employ representation learning to train a feature extractor using the loss function proposed by Wang and Isola [82]. Then we privately fine-tune the model on CIFAR-10.

B.2 Hyperparameter Sweeps

For vision transformer models, we sweep over 5 learning rates {0.1, 0.05, 0.025, 0.0125, 0.00625} for both linear probing (LP), fine-tuning (FT), and first-linear-probing-then-finetuning (LP-FT). Other models are empirically not sensitive to learning rates and we only sweep over 3 learning rates {0.1, 0.05, 0.025}.